15

Photo-Induced Electron Transfer from Dye or Quantum Dot to TiO_2 Nanoparticles at Single Molecule Level

King-Chuen Lin and Chun-Li Chang
Department of Chemistry, National Taiwan University, Taipei 106, Institute of Atomic and Molecular Sciences, Academia Sinica, Taipei 106, Taiwan

1. Introduction

Dye-sensitized solar cell (DSSC) has attracted wide attention for the potential application to convert sunlight into electricity. Organic dyes blended with TiO_2 nanoparticles (NPs) have been recognized as important light harvesting materials especially in the visible spectral range (Hara et al., 2002; Bisquert et al., 2002; Gratzel, 2001; Ferrere & Gregg, 2001; Hagfeldt & Gratzel, 2000; Cahen et al., 2000). The functional materials are assembled in a sandwiched type to undergo photon-induced current process. Following photoexcitation, the embedded dye molecules may lead to electron transfer (ET) to the TiO_2 conduction band. The injected electron flows through the semiconductor network and the external load to the counter electrode. At the counter electrode, the oxidized dye is reduced by electron donation from an electrolyte, and then the circuit becomes complete. The electron transfer kinetics in most dye/TiO_2 systems is as rapid as in the time regime of femtosecond to several hundred picoseconds. The injected electrons are localized in either subband or surface states of TiO_2 semiconductor. A fraction of the electrons, detrapped thermally from the reduced semiconductor, may possibly undergo recombination with the oxidized dye molecules. Such a back ET process takes place slowly from subnanoseconds to several milliseconds. An efficient solar cell deign should control lowering the rate of back electron transfer to prolong the lifetimes of charge-separated states. Therefore, characterizing kinetics of the forward and backward ET may be conducive to facilitating the working efficiency of a solar cell design.

Among a variety of DSSC designs, Grätzel and coworkers have applied ruthenium-based dyes adsorbed on the TiO_2 thin film, thereby achieving a very high power-conversion efficiency >11% (Gratzel, 2003, 2005). Despite a much lower efficiency in comparison, quantum dots (QDs) adopted recently to substitute for dyes have been popularly investigated including PbS (Plass et al., 2002; Ju et al., 2010), InAs (Yu et al., 2006), CdSe (Lee & Lo, 2009; Fan et al., 2010), CdS (Baker & Kamat, 2009; Lee & Lo, 2009), and PbSe (Luther et al., 2008; Choi et al., 2009). QDs have potential to be an alternative as electron donors (Robel et al., 2006; Kamat, 2008), for their unique properties such as size-dependent tunable energy gap (Yu et al., 2003; Kamat, 2008), a broad absorption band with large absorption cross sections (Yu et al., 2003), and multiple exciton generation (Yu et al., 2003; Luther et al., 2007; Kim et al., 2008; Sambur et al., 2010). When QDs absorb a photon to form an electron-hole

pair, the electrons may have chance to transfer to an accepting species such as TiO_2, if the conduction band edge of QDs is tuned higher than the conduction band of TiO_2 (Robel et al., 2006; Yu et al., 2006; Kamat, 2008). Like the DSSC mechanism, kinetic behavior of ET between QDs and TiO_2 is one of the key roles to achieve a high energy-conversion efficiency. The bulk measurements yield ensemble-averaged information and sometimes could mask or overlook specific phenomena occurring at the sensitizer-semiconductor interfaces. For instance, conformation change and reorientation of the adsorbate structure feasibly induce the fluctuation of fluorescence decay times for ET processes, but such detailed dynamical complexity can not be visualized in ensemble experiments (Moerner & Fromm, 2003; Michalet et al., 2006). As a result, single molecule spectroscopy (SMS) has emerged as a powerful tool for investigating the dynamic processes of excited molecules in heterogeneous surrounding (Xie & Dunn, 1994; Garcia-Parajo et al., 2000; Moerner & Fromm, 2003; Michalet et al., 2006; Gaiduk et al., 2007). Analysis of fluorescence intermittency observed in SMS, or called on/off blinking phenomena, has been widely studied to unveil the dynamic behaviors of triplet state (Yip et al., 1998; Veerman et al., 1999; Kohn et al., 2002), molecular reorientation (Ambrose et al., 1994), energy transfer (VandenBout et al., 1997; Cotlet et al., 2005; Flors et al., 2007), spectral diffusions (Xie & Dunn, 1994; Kulzer et al., 1997), and electron transfer (Holman & Adams, 2004; Bell et al., 2006; Wang et al., 2009; Chen et al., 2010). This chapter is confined to understand ET dynamics of either dyes or QDs adsorbed on the TiO_2 NPs thin film at a single molecule level.

By taking advantage of the SMS merits, the IFET phenomena of oxazine 1 dye and CdSe/ZnS core/shell QD adsorbed individually on the TiO_2 NPs surface are demonstrated. We acquired fluorescence trajectories of single dye molecule, characteristic of "on" and "off" blinking with time, in which the intensity fluctuation is attributed to the interfacial electron transfer (IFET) behavior. The fluorescent dye molecule lies in an off-blinking state when its electron moves to the TiO_2 NPs conduction band. While the electron transfers back to the oxidized state, the dye molecule blinks on again following photoexcitation. Discrete fluorescence intensity jumps between "on" and "off" level are analyzed by using autocorrelation function. The "on" and "off" lifetimes and the subsequent rate constants of forward and backward ET are then determined. On the other hand, the fluorescence lifetimes of QDs are measured as an alternative determination for the ET rate constants. QDs with different sizes are adopted for demonstration. We apply time-correlated single-photon counting (TCSPC) to measure fluorescence lifetimes among a quantity of QDs for each size. The fluorescence lifetime becomes shorter and the resultant "off" time is prolonged with decreased size of QDs. The off-time and on-time probability densities are then estimated and fitted appropriately. With the aid of Marcus model, theoretical ET rate constants are calculated for comparison and the ET process may thus be gained insight.

2. Experimental

2.1 Apparatus

All single molecule experiments were performed with a confocal fluorescence microscope. For the single dye (or QD) experiments, a single-mode pulsed laser at 630 nm (or 375 nm), with a repetition rate of 10 MHz (or 5 MHz) and pulsed duration of 280 ps (or 300 ps), was used as the excitation source. The beam collimated with a pair of lenses was spectrally filtered with an excitation filter before entering an inversed microscope. An oil immersion objective (100x, NA1.40) was used both to focus the laser beam onto the sample, prepared

on the surface of a glass coverslip, and to collect fluorescence from the sample. The excitation intensity of the pulsed beam was constantly measured to be 40 - 210 W/cm^2 right on the top of the bare coverslip throughout the experiments. The fluorescence, after transmitting through a dichroic mirror, was refocused by a tube lens (200 mm focal length) onto an optical fiber (62.5 μm diameter) which was coupled to an avalanche photodiode (APD) detector with a 175 μm active area. Here the fiber serves as a pinhole to reject out-of-focus light. The fluorescence signal may also be reflected simultaneously to a charge-coupled device (CCD) by a beamsplitter. A notch filter (6<OD) or a combination of bandpass filters were positioned in front of the detector to remove excitation background. Given the wide-field images with a CCD detector, each fluorescent single molecule was readily moved to an illuminated position using a x-y positioning stage. The fluorescence lifetime of single molecule was measured by TCSPC with a TimeHarp 200 PCI-board (PicoQuant). The data were stored in a time-tagged time-resolved mode, which allowed recording every detected photon and its individual timing information. By taking into account deconvolution of the instrument response function (SymPhoTime by PicoQuant), the TCSPC curve was analyzed by single exponential tail-fit.

2.2 Material preparation

The TiO_2 precursor was prepared by a sol-gel process. 72 mL of 98% Titanium(IV) isopropoxide was added to 430 mL of 0.1 M nitric acid solution which was then stirred and heated to 85 ^oC for 8 h. The colloid, as filtered from the cooled mixture, was heated again in an autoclave at five temperatures of 180, 200, 220, 240, and 260 ^oC for 12 h to grow TiO_2 NPs. The TiO_2 colloid was concentrated to 13 wt%, followed by addition of a 30 wt% (with respect to TiO_2) of polyethylene glycol to prevent from cracking during drying.

To prepare for the thin film, 40-50 μL of 0.65% TiO_2 NPs aliquot was spin-coated on a cleaned coverslip. The same process was repeated four times to ensure TiO_2 well coated over the coverslip. After drying in the air for 30 min, the film was heated to 450 ^oC at a rate of 20 ^oC/min, and remained for 30 min before cooling to the room temperature. The phase and the size of TiO_2 NPs were characterized by using scanning electron microscopy. A drop of 30 μL of 0.1 nM oxazine 1 dye in methanol solution or 35 μL of 4 - 200 pg/L QDs in toluene solution was spin-coated over the TiO_2 NPs surface, and then put on the sample stage of microscope for fluorescence measurement.

3. Fluorescence intermittency and electron transfer by single dye molecule

3.1 Fluorescence lifetimes

As shown in Fig.1, the TiO_2 NPs thin film was well covered over the coverslip to ensure that the oxazine 1 dye may be fully adsorbed on the TiO_2 surfaces. The enlarged images displayed the NPs size about ~20 nm. Fig.2 shows absorption spectra of oxazine 1 solution in the presence (or absence) of TiO_2 NPs by means of ensemble measurements. The absorption cross section reaches as large as ~$3.5x10^{-16}$ cm^2 at 630 nm. The fluorescence yield is 0.11 in ethanol as the solvent and increases to 0.19 in ethylene glycol (Sens & Drexhage, 1981). When the dye in methanol solution is diluted from 10^{-6} to 10^{-8} M, the spectral profile remains the same with a major peak and a minor shoulder. The spectra appear almost the same between the conditions with and without TiO_2 NPs involvement. The results suggest that the dimer contribution should be minor and negligible.

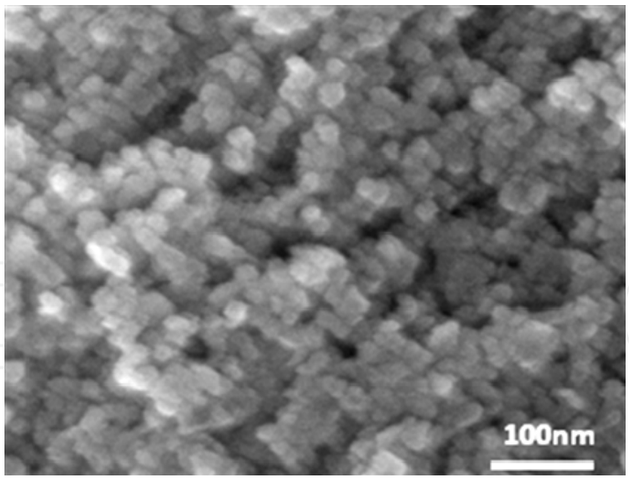

Fig. 1. Images of TiO_2 NPs thin film by using scanning electron microscopy. The average sizes of TiO_2 NP are about 20 nm for both films.

A 10^{-10} M of oxazine 1 dye solution was spin-coated on a bare or a TiO_2 NPs-coated coverslip. Fig.3(a) displays the fluorescence images of the single oxazine 1 molecules within a 24 μm x 24 μm area on the bare coverslip, as excited by a pulsed laser at 630 nm with excitation intensity of 39±2 W/cm². Each bright spot is attributed to a single molecular fluorescence. The diffraction-limited spot size is about ~650 nm. Fig.3(b) shows the background emissions of the TiO_2 NPs surface. Stray light scattered by the TiO_2 NPs causes background noise, which is however dimmer than those fluorescent spots from the dye molecules. Fig.3(c) shows the single molecular fluorescence images of dye molecules on TiO_2 NPs surface. The maximum fluorescence intensity reaches 650 counts acquired by a CCD within an integration time of 0.5 s. The fluorescent spots have different intensities resulting from variation of molecular orientation and micro-environments. The surface densities of fluorescent oxazine 1 on glass or TiO_2 coverslip are counted to be 0.088 or 0.085 per μm², respectively, with an uncertainty of ±10%. It is difficult to make a comparison with the surface density prepared initially, since a great amount of dye solution is sputtered away during the spin-coating process. The roughness of the TiO_2 NPs-coated coverslip may reduce the dye molecules from sputtering away to some extents, as compared to a smooth bare glass. Although the surface density of fluorescent spots is similar between them, some molecules in the excitation might be quenched by a faster IFET process before fluorescing and thus fail to be detected. The clefts or interstices in the TiO_2 film are probably ideal sites for effective IFET.

As shown in Fig.4(a), fluorescence decay of a single dye molecule on TiO_2 is obtained for the lifetime measurements by the TCSPC method. The decay curve is fitted to a single exponential function yielding a lifetime of 2.6 ns. In this manner, the lifetimes successively determined among 100 different oxazine 1 molecules are distributed in Fig.4(b), with an average value of 2.86±0.31 ns. The lifetime scattering reveals an inhomogeneous character among the dye molecules measured, because of variation of dipole orientation, transition frequency, and molecular polarization on the surface. In addition, the fluctuation of the lifetime is partially attributed to the power density variation which is about ±3%. For comparison, the average lifetimes over 100 oxazine 1 molecules are measured analogously to be 3.02±0.61 ns on the bare coverslip.

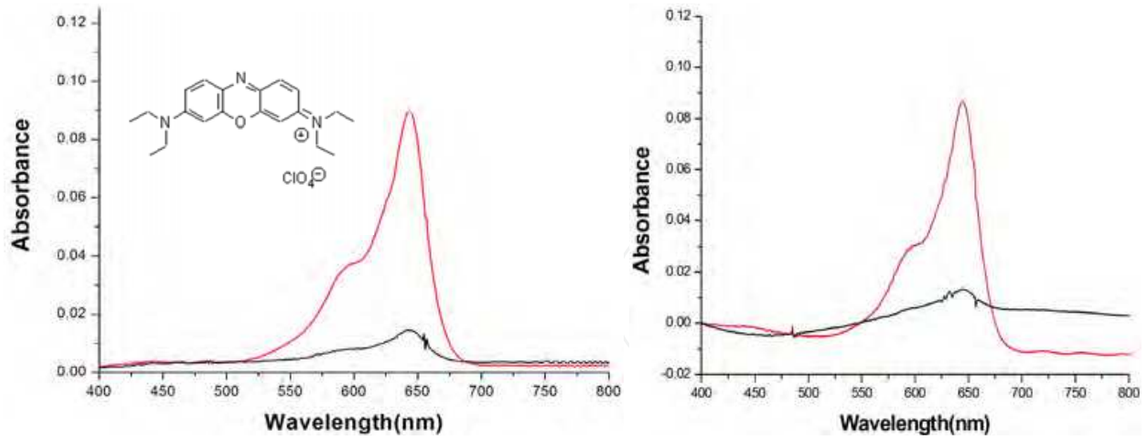

(a) (b)

Fig. 2. (a) Absorption spectra of oxazine 1 dye in methanol solution with concentration of $1x10^{-6}$ (larger peak) and $1x10^{-8}$ M, respectively. Oxazine 1 structure is also displayed. (b) Absorption spectra of oxazine 1 methanol solution with concentration of $1x10^{-6}$ (larger peak) and $1x10^{-8}$ M, respectively, in the presence of TiO_2 NPs

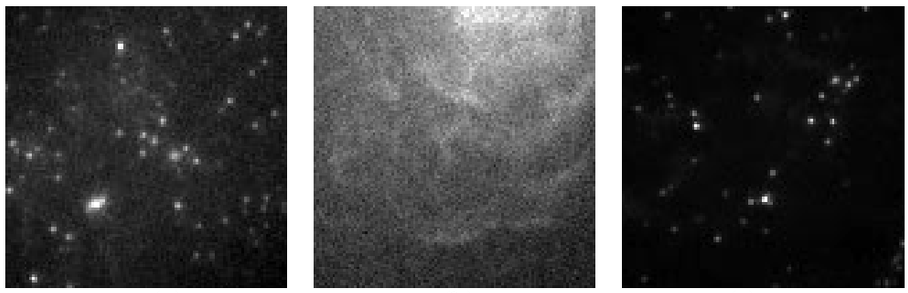

(a) (b) (c)

Fig. 3. Fluorescence images of (a) oxazine 1 molecules on bare coverslip, (b) TiO_2 NPs film without dye molecules involved, and (c) oxazine 1 molecules on TiO_2 NPs–coated coverslip.

Despite no statistical difference with the uncertainty considered, the average lifetime of the dye on the TiO_2 film is significantly smaller than that on the bare coverslip. While inspecting Fig.4(b), the asymmetric distribution shows more molecules lying on the side of shorter fluorescence lifetime. It suggests two points. First, some molecules might undergo even faster IFET process such that the excited state lifetimes become too short to be detected. Second, slight difference of the fluorescence lifetimes implies that most IFET processes should be slow and inefficient. The oxazine 1 molecule lacks effective anchoring groups like carboxylate in metal-polypyridine complexes to covalently bind the dye to the semiconductor (Oregan & Gratzel, 1991; Ramakrishna et al., 2005). These dye molecules randomly selected are anticipated to be physisorbed to the TiO_2 NPs surface or loosely trapped at the NPs interstices. However, that does not mean all interactions based on physisorption can not lead to efficient electron transfer. Some organic dyes such as cyanine or xanthene dyes incorporated in Langmuir-Blodgett films deposited on In_2O_3 or SnO_2 electrodes show very efficient electron transfer even without chemisorptions, due to a large free-energy difference between the lowest unoccupied molecular orbital (LUMO) of the dye

and the edge of the conduction band of the semiconductor(Arden & Fromherz, 1980; Biesmans et al., 1991; Biesmans et al., 1992).

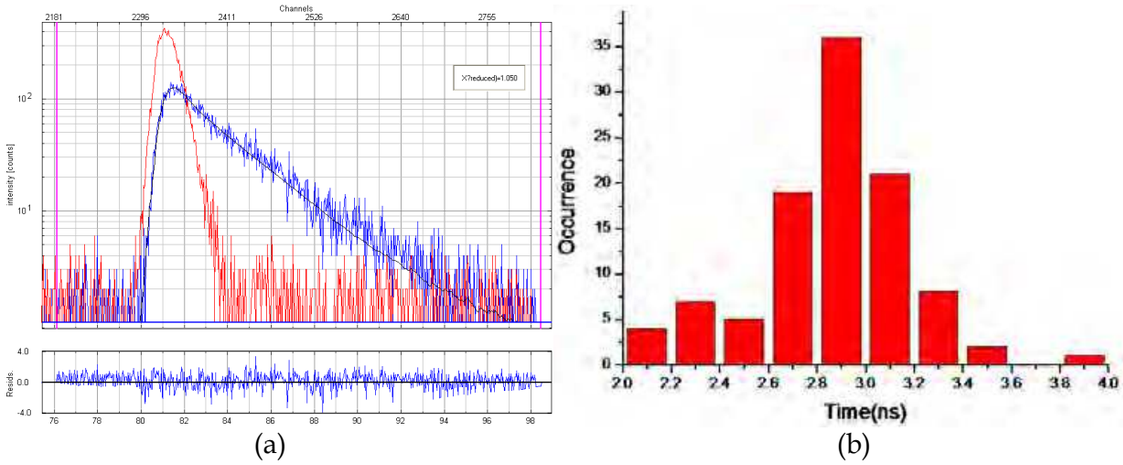

Fig. 4. (a) Fluorescence decay of single oxazine 1 molecule in the presence of TiO_2 NPs measured by using time-correlated single photon counting. The instrument response function gives a faster decay estimated to be 550 ps. (b) Distribution of excited state lifetimes among 100 single oxazine 1 molecules on the TiO_2 NPs surface, yielding an average lifetime of about 2.86 ns.

3.2 Fluorescence intensity trajectories

Fig.5(a) displays fluorescence intensity as a function of running time of a single oxazine 1 molecule on the bare coverslip with a 20 ms binning time to record the photon counts of emission. These time scales average out any faster fluorescence fluctuation or blinking of the dye molecules. The single-molecule trace shows a constant level of fluorescence intensity which then drops to the background in one step when photobleaching occurs. Wilkinson et al. reported the triplet state lifetime to be 14.5 μs for oxazine 1 in acetonitrile solution (Wilkinson et al., 1991), and a significantly longer lifetime is yet expected for the dye adsorbed on the solid film. A constant level of fluorescence intensity in Fig.5(a) implies that the prolonged lifetimes should be much shorter than the integration time adopted such that the triplet blinking may be smeared out. When 100 single molecules are sampled, about 70% display the trajectories like Fig.5(a). The remaining show blinks occasionally before photobleaching, in part because of photo-induced electron transfer to impurity sites of the glass coverslip. It is difficult to observe clearly triplet blinking of the single molecule caused by intersystem crossing. Instead, an average intensity of 5 counts/20 ms appears. The triplet state lifetime if assumed to be 14.5 μs amounts to 0.003 count, which is too weak to be resolved temporally.

As shown in Fig.6A(a), when the single-molecule fluorescence intensity trajectory of the dye molecules on the bare coverslip is slotted within 1 s-window, the fluorescence decay lifetimes are measured to be 3.63 ns and 3.59 ns for the time period of 54~55s and 266~267s, respectively (Fig.6A(b)). Alternatively, the lifetime fluctuation trajectory binned in 0.5 s-window gives rise to an average lifetime of 3.44±0.48 ns (Fig.6A(c)), which is consistent with that averaged over 100 molecules. These facts indicate that the fluorescence intensity fluctuation for oxazine 1 on glass is dominated by the radiative relaxation process from the singlet state.

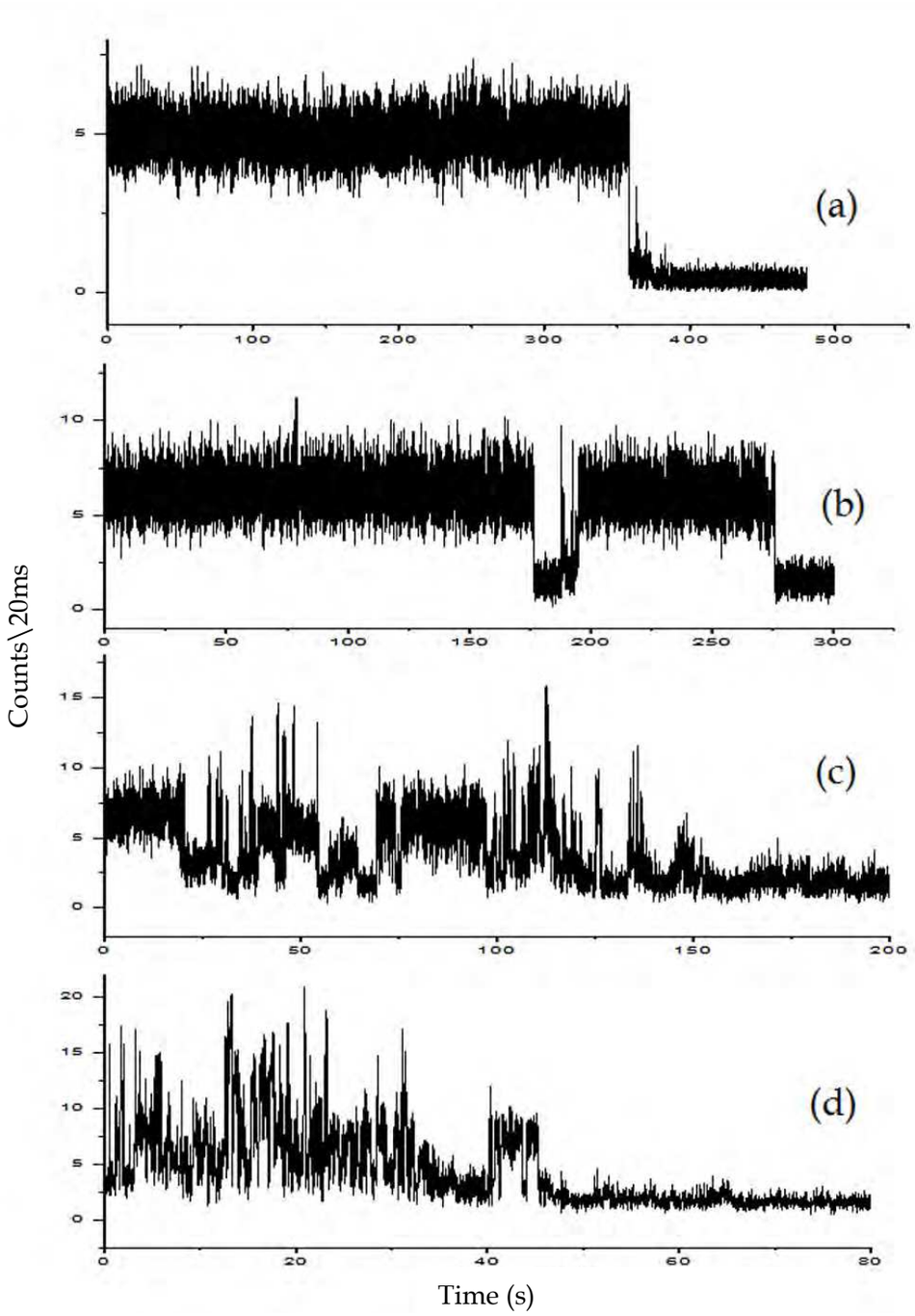

Fig. 5. Fluorescence trajectories recorded for single oxazine 1 molecules (a) on bare coverslip, and (b-d) on TiO_2 NPs-coated coverslip.

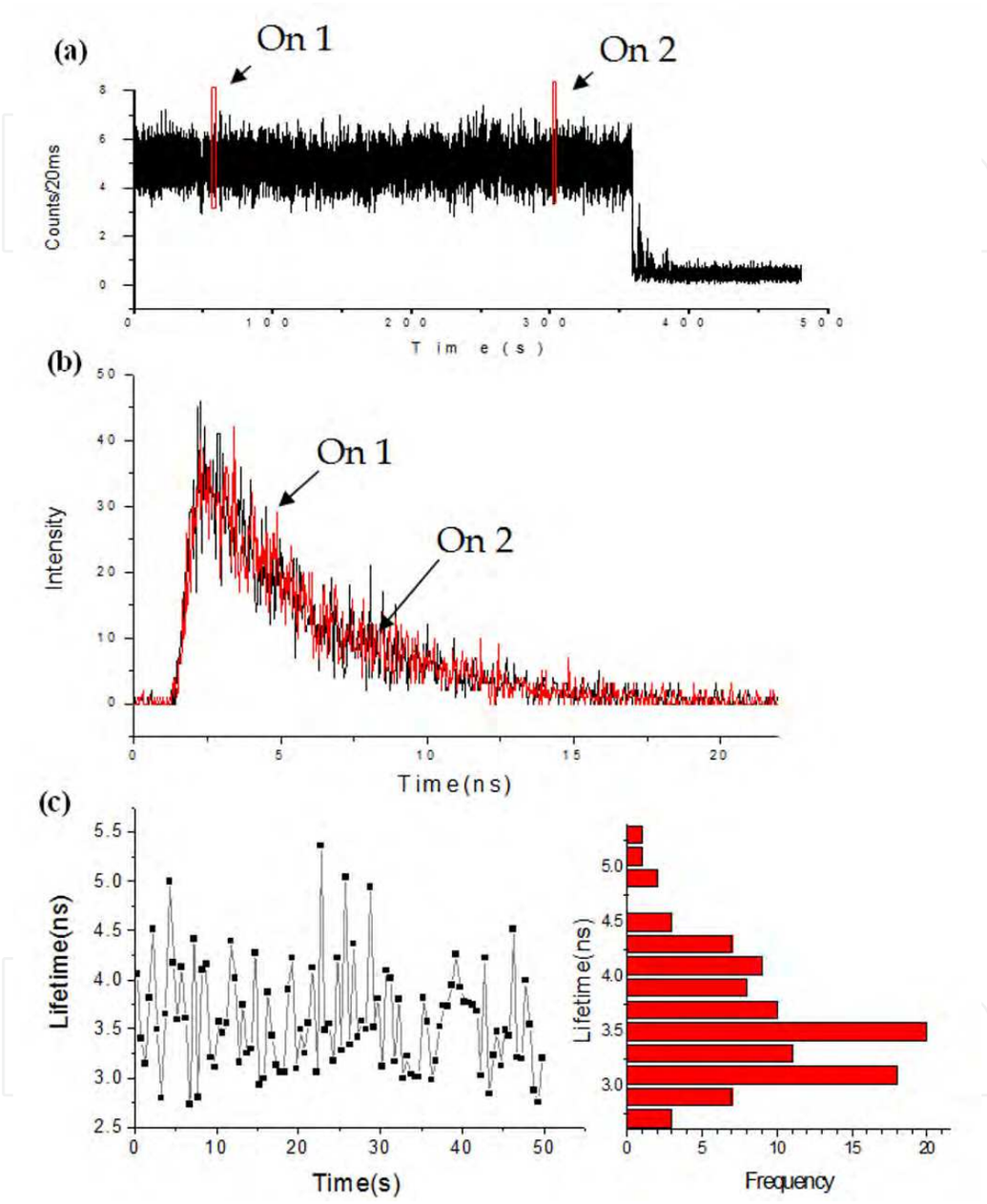

Fig. 6. (A) Single-molecule fluorescence decay profile of oxazine1 on bare glass. (a) The fluorescence intensity fluctuation slotted at 1 and 2 positions each within 1-s window. (b) Fluorescence decay profile for the 1 and 2 slots gives rise to the decay time of 3.63 ns and 3.59 ns, respectively. (c) The lifetime (binning window 0.5s) fluctuation trajectory (left), and the histogram for the lifetime trajectory from 0 to 50 s before photobleaching. The average lifetime is 3.44±0.48 ns.

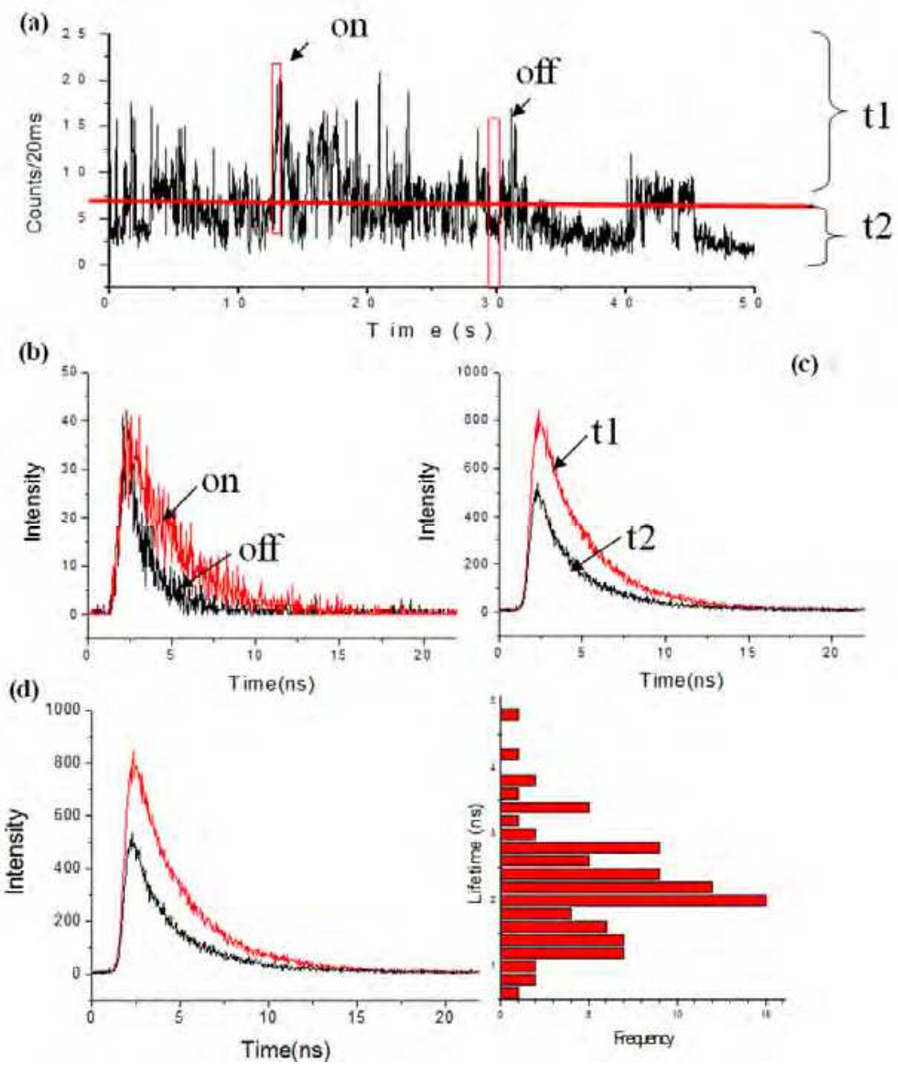

Fig. 6. (B) Single-molecule fluorescence decay profile of oxazine1 on TiO_2 NPs film. (a) The fluorescence intensity fluctuation slotted at one "on" position and the other "off" position. (b) Fluorescence decay profile for the "on" and "off" slots gives rise to the decay time of 2.93 and 1.26 ns, respectively. (c) Given a threshold set at 7 photocounts/20 ms, the emission trajectory is separated to higher level and lower level. Fluorescence decay profiles for high and low intensity have similar results as the "on" and "off" slots in (b). (d) The lifetime (binning window 0.5s) fluctuation in a range from 0.6 to 4.8 ns (left), and the histogram for the lifetime trajectory from 0 to 50 s before photobleaching.

On the other hand, Fig.5(b-d) show the fluorescence trajectories of individual dye molecules in the presence of TiO_2 NPs thin film ranging from several microseconds to seconds before photobleaching. These trajectories are classified into three types among 100 single dye molecules as sampled. About 20% of molecules yield the traces as in Fig.5(b), in which the interaction with TiO_2 NPs is weak such that the molecule fluoresces at most time. A 60% majority show the traces as in Fig.5(c), in which a stronger interaction is found and the "off" time becomes longer. The remaining 20% give the traces as in Fig.5(d), in which the

molecule stays longer at "off" time. The molecule in Fig.5(d) should have relatively active electron transfer such that the fluorescence process is suppressed.

Fig.5(d) is used as an example. The fluorescence intensity trajectory is slotted within a 500-photon binned window to select one "on" intensity and the other "off" intensity (Fig.6B(a)). Analyzing the fluorescence decay yields a result of 2.93 and 1.26 ns for the "on" (12.85~13.33 s slot) and "off" (29.15~30.20 s slot) lifetime, respectively (Fig.6B(b)). Given a threshold at 7 counts/20 ms, the fluorescence intensity is divided to higher level and lower level. The lifetime analysis of these two levels yields the results similar to those obtained in the above time slots. The "on" state shows a twofold longer lifetime than the "off" state (Fig.6B(c)). This fact indicates that the fluorescence intensity fluctuation is caused by both factors of reactivity, i.e., the fraction of IFET occurrence frequency (Wang et al., 2009), and rate of electron transfer. The fluorescence lifetimes analyzed within 0.5s-window fluctuate in a range from 0.6 to 4.8 ns, which is more widely scattered than those acquired on the bare glass (Fig.6B(d)). This phenomenon suggests existence of additional depopulation pathway which is ascribed to ET between oxazine1 and TiO_2. However, other contribution such as rotational and translational motion of the dye on the TiO_2 film can not be rule out without information of polarization dependence of the fluorescence.

3.3 Autocorrelation analysis

An autocorrelation function based on the fluorescence intensity trajectory is further analyzed. When the dye molecules are adsorbed on the TiO_2 NPs surface, a four-level energy scheme is formed including singlet ground, singlet excited, and triplet states of the dye molecule as well as conduction band of TiO_2. Upon irradiation with a laser source, the excited population may undergo various deactivation processes. Because the selected dye molecule has a relatively short triplet excursion, the fluorescence in the absence of TiO_2 film becomes a constant average intensity with near shot-noise-limited fluctuation, as displayed in Fig.5(a) (Haase et al., 2004; Holman & Adams, 2004). As a result, the system can be simplified to a three-level energy scheme.

As the ET process occurs, the fluorescence appears to blink on and off. The transition between the on and off states may be considered as feeding between the singlet and the conduction subspaces (Yip et al., 1998),

$$\text{On} \underset{k_{on}}{\overset{k_{off}}{\rightleftharpoons}} \text{off} . \tag{1}$$

The on-state rate constant is equivalent to the backward ET rate constant from the conduction band, i.e.,

$$k_{on} = k_{bet} , \tag{2}$$

while the off-state rate constant corresponds to the excitation rate constant k_{ex} multiplied by the fraction of population relaxing to the conduction band, as expressed by

$$k_{off} = \frac{k_{et}}{k_{21} + k_{et}} k_{ex} . \tag{3}$$

Here, k_{21} is the relaxation rate constant from the excited singlet to ground state containing the radiative and non-radiative processes and k_{et} is the forward ET rate constant. k_{ex} is related to the excitation intensity I_o (units of erg/cm^2 s) by

$$k_{ex}=\sigma I_o/h\upsilon, \tag{4}$$

where σ is the absorption cross section and hυ is the photon energy. The average residence times in the on and off states correspond to the reciprocal of the feeding rate in the off and on states, respectively. That is, $\tau_{on} = 1/k_{off}$ and $\tau_{off} = 1/k_{on}$.
The rate constants in on-off transition may then be quantified by analyzing autocorrelation of fluorescence intensities (Holman & Adams, 2004). The normalized autocorrelation function is defined as the rate of detecting pairs of photons separated in time by an interval τ, relative to the rate when the photons are uncorrelated. It is expressed as

$$G(\tau) = \frac{< I(t)I(t+\tau) >}{< I(t) >^2}\ , \tag{5}$$

where I(t) is the fluorescence intensity at time t and τ is the correlation time. The bracketed term denotes the intensity average over time. When the population relaxation is dominated by the singlet decay, the autocorrelation function may be simplified to an exponential decay, i.e.,

$$G(\tau) = A + Be^{-k\tau}\ , \tag{6}$$

where A is an offset constant, B a pre-exponential factor, and k the decay rate constant. They are determined by fitting to the autocorrelation data. These parameters are explicitly related to the phenomena of on/off blinking due to the ET processes by,

$$k = k_{on} + k_{off} \tag{7}$$

and

$$\frac{B}{A} = \frac{k_{on}k_{off}(I_{on} - I_{off})^2}{(k_{on}I_{on} + k_{off}I_{off})^2}\ . \tag{8}$$

If I_{on}>>I_{off}, then the above equation is simplified to

$$\frac{B}{A} = \frac{k_{off}}{k_{on}}\ . \tag{9}$$

The forward and backward ET rate constants in the dye molecule-TiO_2 NPs system can thus be evaluated.
According to eq.5, Fig.7(a) shows that the autocorrelation result based on the fluorescence trajectory of the dye on glass (Fig.5(a)) appears to be noisy ranging from zero to microseconds. The dynamic information of the triplet state can not be resolved, consistent with the analyzed results of fluorescence decay times. When the dye molecule is on TiO_2, the fluorescence trajectory given in Fig.5(c) is adopted as an example for evaluation of the individual "on" and "off" times. As shown in Fig.7(b), the resulting autocorrelation function

is fitted to a single exponential decay, yielding a B/A value of 0.2 and k of 2.17 s^{-1}. Given the excitation rate constant k_{ex} of $2.2x10^4$ s^{-1} (38.5 W/cm^2 was used) and the fluorescence decay k_{21} of $3.28x10^8$ s^{-1} determined in the excited state lifetime measurement, k_{et} and k_{bet} are evaluated to be $5.4x10^3$ and 1.8 s^{-1}, respectively, according to eqs.2,3,7, and 9. The IFET and back ET rate constants with the "on" and "off" times for the examples in Fig.5(b-d) are listed in Table 1. For comparison, the corresponding lifetime measurements are also listed. A more efficient IFET is apparently accompanied by a shorter excited state lifetime.

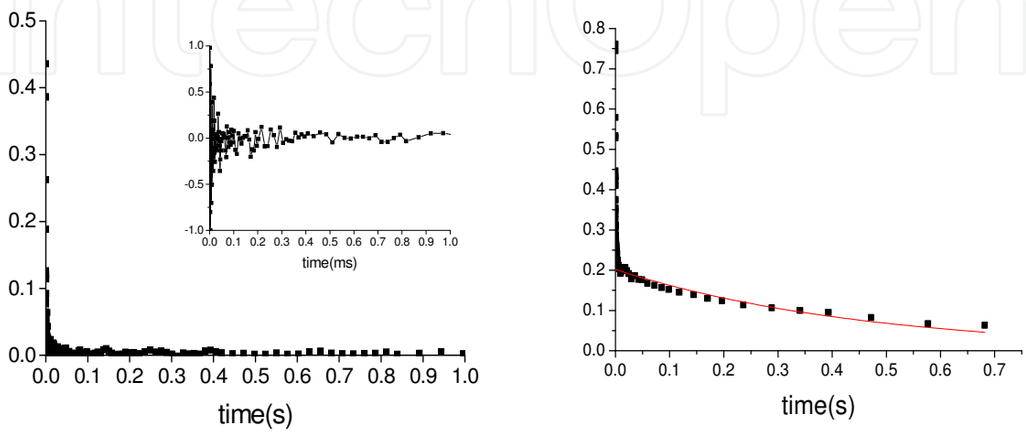

(a) (b)

Fig. 7. Autocorrelation function of fluorescence intensity from single oxazine 1 molecules (a) on bare coverslip, (b) on TiO_2 NPs-coated coverslip. The inset in (a) is the enlarged trace within the range of 1 ms.

	Lifetime/ns	τ_{on} (s)	τ_{off} (s)	k_{et} (s^{-1})	k_{bet} (s^{-1})
A	**4.0**	**-**	**-**	**-**	**-**
B	**3.4**	**86.02**	**1.43**	**$1.6 x10^2$**	**0.7**
C	**3.1**	**2.75**	**0.55**	**$5.4 x10^3$**	**1.8**
D	**2.9**	**0.49**	**0.08**	**$3.2 x10^4$**	**12.0**

Table 1. The excited state lifetimes and kinetic data for the single-molecule traces shown in Fig. 6.

As with the above examples, 100 single dye molecules are successively analyzed. The resulting IFET and back ET rate constants are displayed in the form of histogram (Fig.8(a) and (b)), yielding a range of 10^2-10^4 and 0.1-10 s^{-1}, respectively. The distributions are fitted with an individual single-exponential function to yield an average value of $(1.0\pm0.1)x10^4$ and 4.7 ± 0.9 s^{-1}, which are the upper limit of the IFET and back ET rate constants among these 100 single molecules analyzed, if the unknown contributions of rotational and translational motion are considered. The obtained average rate of electron transfer is much slower than the fluorescence relaxation. That is why no statistical difference of the fluorescence lifetimes of the dye is found between TiO_2 and bare coverslip. The ET rate constant distribution could be affected by different orientation and distance between dye molecule and TiO_2 NPs. The weak coupling between electron donor and acceptor may be caused by physisorption

between the dye molecule and the TiO_2 NPs or a disfavored energy system for the dye electron jumping into the conduction band of the semiconductor. The resulting ET quantum yield as small as $3.1x10^{-5}$ is difficult to be detected in the ensemble system. Nevertheless, such slow electron transfer events are detectable at a single molecule level as demonstrated in this work.

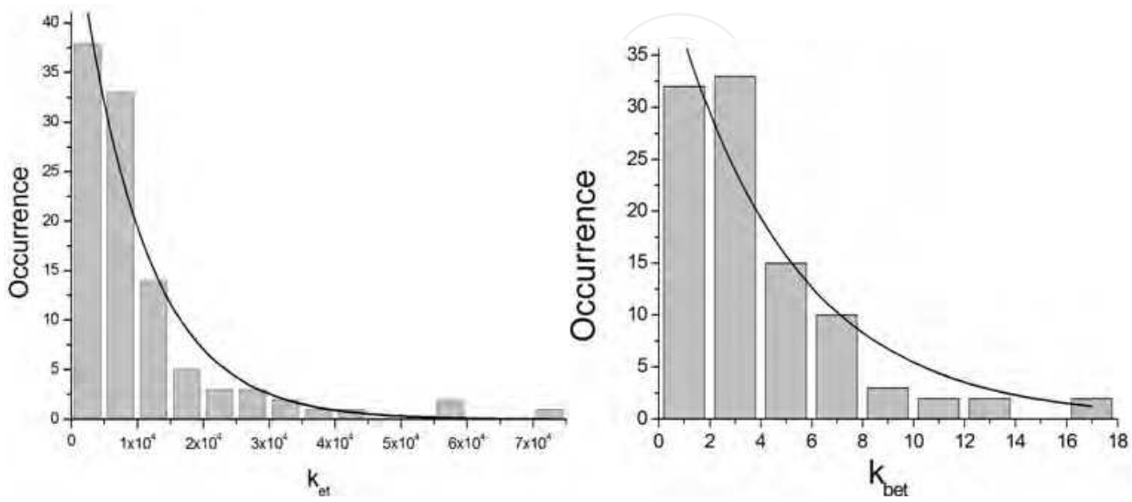

(a) (b)

Fig. 8. The histograms of (a) k_{et} and (b) k_{bet} determined among 100 dye molecules. The average values of $(1.0\pm0.1)x10^4$ and 4.74 s^{-1} are evaluated by a fit to single-exponential function.

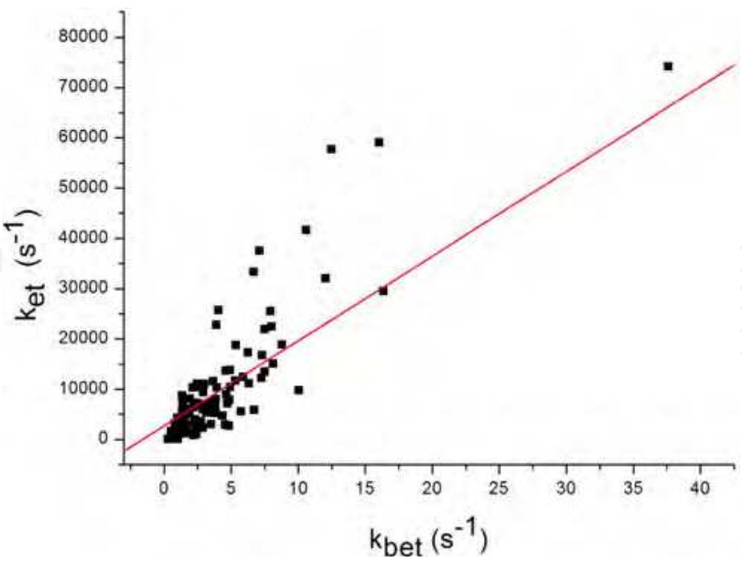

Fig. 9. A linear correlation between photo-induced electron transfer and back electron transfer rate constant.

The process of photo-induced ET involves charge ejection from the oxazine 1 LUMO (~2.38 ev) into a large energetically accessible density of states within the conduction band of

TiO_2(~4.4 ev), while the back ET involves thermal relaxation of electrons from the conduction band or from a local trap (energetically discrete states) back to the singly occupied molecular orbital (SOMO) of the oxazine 1 cation.[37] It is interesting to find a linear correlation with a slope of $1.7x10^3$ between IFET and back ET rate constants, as shown in Fig.9. Despite difference of the mechanisms, k_{bet} increases almost in proportion to k_{et}. Such a strong correlation between forward and backward ET rate constants suggests that for different dye molecules the ET energetics remains the same but the electronic coupling between the excited state of the dye molecules and the conduction band of the solid film varies widely (Cotlet et al., 2004). Both forward and backward ET processes are affected similarly by geometric distance and orientation between electron donor and acceptor.

4. Fluorescence intermittency and electron transfer by quantum dots

4.1 Fluorescence intermittency and lifetime determination

Three different sizes of CdSe/ZnS core/shell QDs were used. Each size was estimated by averaging over 100 individual QDs images obtained by transmission emission spectroscopy (TEM), yielding the diameters of 3.6±0.6, 4.6±0.7, and 6.4±0.8 nm, which are denoted as A, B, and C size, respectively, for convenience. Each kind was then characterized by UV/Vis and fluorescence spectrophotometers to obtain its corresponding absorption and emission spectra. As shown in Fig.10(a) and (b), a smaller size of QDs leads to emission spectrum shifted to shorter wavelength. From their first exciton absorption bands at 500, 544, and 601 nm, the diameter for the CdSe core size was estimated to be 2.4, 2.9, and 4.6 nm (Yu et al., 2003), respectively, sharing about 25-37% of the whole volume. In addition, given the band gaps determined from the absorption bands and the highest occupied molecular orbital (HOMO) potential of -6.12 ~ -6.15 Ev (Tvrdy et al., 2011), the LUMO potentials of QDs may be estimated to be -4.06, -3.86, and -3.67 eV along the order of decreased size.

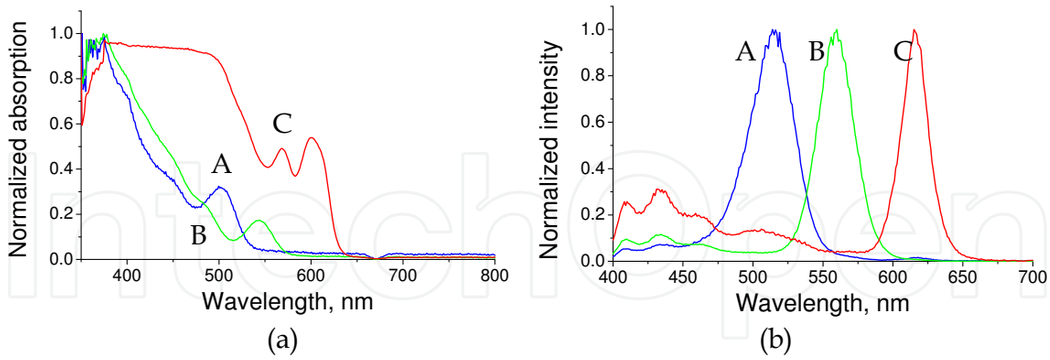

Fig. 10. (a) Absorption and (b) fluorescence spectra of QDs in toluene solution with excitation wavelength fixed at 375 nm. The maximum intensities for both spectra have been normalized. A, B, and C species have the diameters of 3.6, 4.6, and 6.4 nm, respectively.

Each size of QDs was individually spin-coated on bare and TiO_2 coverslip. Fig.11 shows an example for the photoluminescence (PL) images within a 24 μm x 24 μm area of the smallest QDs on the glass and TiO_2 NPs thin film, as excited at 375 nm. The surface densities of fluorescent QDs on TiO_2 were less than those on glass. Their difference becomes more significant with the decreased size of QDs.

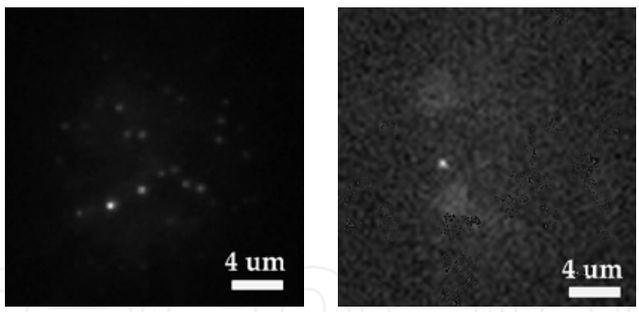

Fig. 11. The CCD images of QDs with the diameter of 3.6 nm at $4.5x10^{-11}$ g/L which was spin-coated on (a) glass and (b) TiO_2 film.

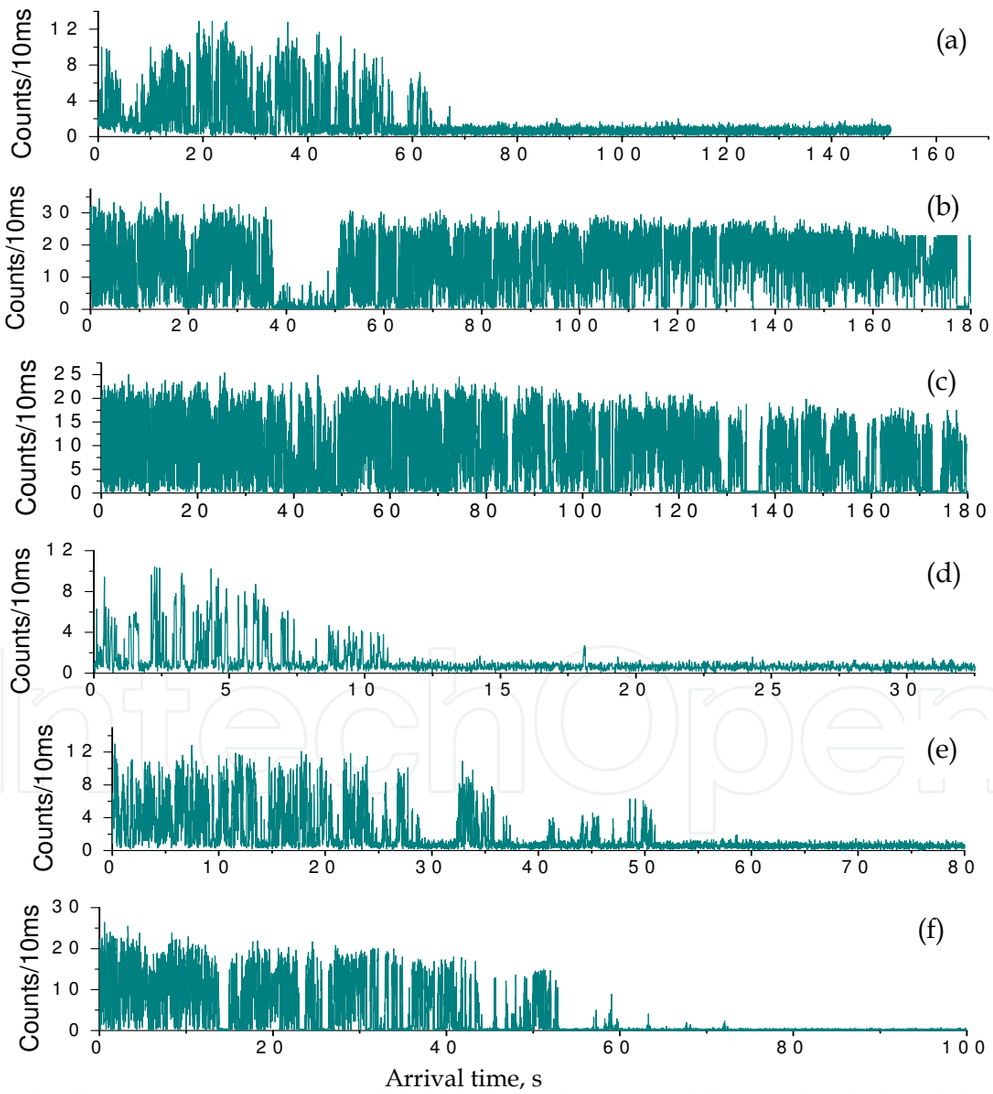

Fig. 12. The fluorescence trajectories of single QD with A, B, and C size adsorbed on (a,b,c) glass and (d,e,f) TiO_2 film. The order of increased size is followed from a to c and from d to f.

As a single bright spot was focused, the trajectory of fluorescence intensity was acquired until photobleaching. The trajectory is represented as a number of emitting photons collected within a binning time as a function of the arrival time after the experiment starts. Fig.12 shows the examples for the three sizes of QDs on glass and TiO_2. The bleaching time of the trajectory appears shorter with the decreased size of QDs, showing an average value of 9.4, 19.6, and 34.1 s on TiO_2, which are much shorter than those on glass. In addition, QDs on either surface are characterized by intermittent fluorescence. As compared to those on glass coverslip, QDs on TiO_2 endure shorter on-time (or fluorescing time) events but longer off-time events. This trend is followed along a descending order of size.

The photons collected within a binning time can be plotted as a function of delay time which is defined as the photon arrival time with respect to the excitation pulse. The fluorescence decay for a single QD is thus obtained. Each acquired curve can be applied to a mono-exponential tail-fit, thereby yielding the corresponding lifetime for a selected arrival time slot. For increasing single-to-noise ratio, the on-state lifetime is averaged over the entire trajectory. However, the off-state lifetime cannot be precisely estimated, because its signal is close to the background noise with limited number of photons collected. Fig.13 shows a single QD lifetime determined for different sizes on glass and TiO_2. A smaller size of QDs results in a shorter on-state lifetime on either surface. Given the same size of QDs, the lifetime on TiO_2 appears to be shorter than that on glass. Their lifetime difference increases with the decreased size. As reported previously (Jin et al., 2010a), the trajectories of fluorescence intermittency and lifetime fluctuation are closely correlated. A similar trend is also found in this work.

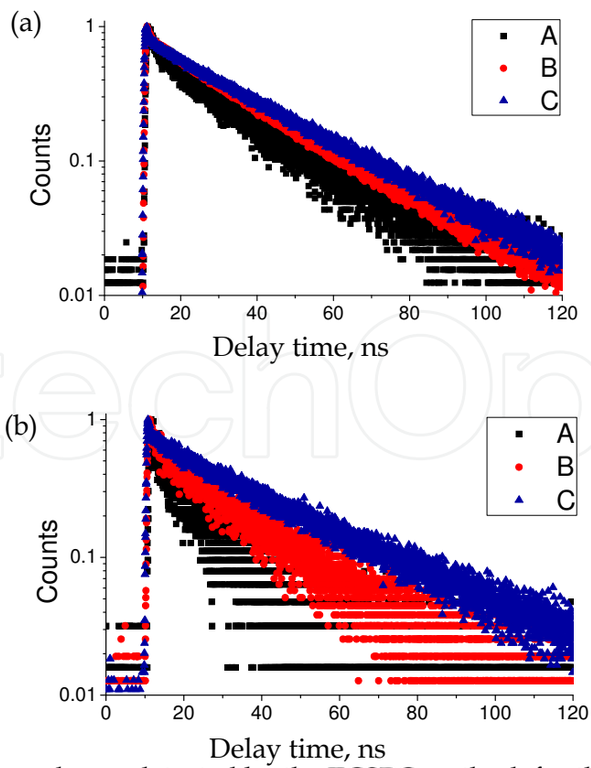

Fig. 13. The fluorescence decay, detected by the TCSPC method, for three types of QDs spin-coated on (a) glass and (b) TiO_2 film. The number of counts is normalized to unity.

Fig.14 shows the lifetime histograms among 20-90 single QDs for the three sizes on glass and TiO_2. The corresponding average lifetimes are listed in Table 2. As shown in Fig.14, the smallest QDs on TiO_2 have much less on-events than those on glass. For clear lifetime comparison of QDs adsorption between glass and TiO_2, each on-event distribution is normalized to unity. The Gaussian-like lifetime histogram has a wide distribution for both glass and TiO_2. The lifetime difference for the A type of QDs can be readily differentiated between these two surfaces. As listed in Table 2, their average lifetimes correspond to 19.3 and 14.9 s. In contrast, a tiny lifetime difference between 25.7 and 25.5 s for the C type of QDs is buried in a large uncertainty.

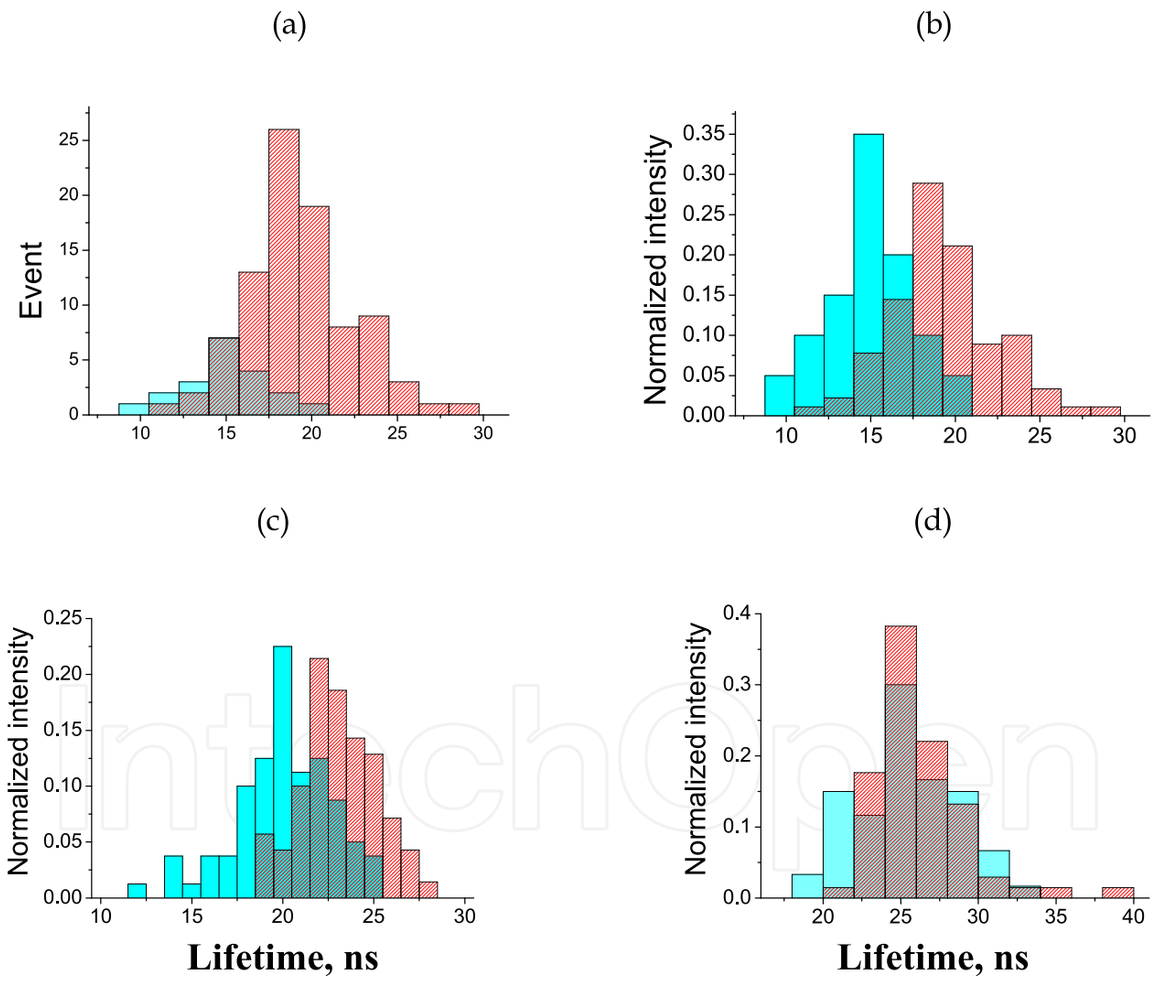

Fig. 14. The distributions of fluorescence lifetime for (a,b) QDs A and (c,d) QDs B and C. (a) comparison of on-event occurrence for QDs A between glass and TiO_2. (b,c,d) each area of distribution is normalized to unity. The lifetime distributions of QDs on glass and TiO_2 are displayed in red and blue, respectively.

Quantum Dots	Size	Substrate	Amount	Lifetime, ns
A	$3.6 \pm 0.6\ nm$	Glass	90	19.3 ± 3.2
		TiO_2 film	20	14.9 ± 2.4
B	$4.6 \pm 0.7\ nm$	Glass	70	22.6 ± 2.1
		TiO_2 film	80	19.6 ± 2.7
C	6.4 ± 0.8 nm	Glass	68	25.7 ± 2.2
		TiO_2 film	60	25.5 ± 3.2

Table 2. Size-dependence of on-state lifetimes of quantum dots (QDs) on glass and TiO_2 film which are averaged over a quantity of single QDs.

4.2 Interfacial electron transfer

Upon excitation at 375 nm, a QD electron is pumped to the conduction band forming an exciton. The energy gained from recombination of electron and hole will be released radiatively or nonradiatively. However, the excited electron may be feasibly scattered out of its state in the conduction band and be prolonged for recombination. The excited electron probably undergoes resonant tunneling to a trapped state in the shell or nonresonant transition to another trapped state in or outside the QD (Hartmann et al., 2011; Krauss & Peterson, 2010; Jin et al., 2010b; Kuno et al., 2001). The off state of QD is formed, as the charged hole remains. When a second electron-hole pair is generated by a second light pulse or other processes, the energy released from recombination of electron and hole may transfer to the charged hole or trapped electron to cause Auger relaxation. Its relaxation rate is expected to be faster than the PL rate. Given a QD with the core radius of 2 nm, the Auger relaxation rate was estimated to be 100 times larger than the radiative decay rate (Hartmann et al., 2011). The fluorescence fluctuation is obviously affected by the Auger relaxation process that is expected to be <100 ps.

As shown in Fig.12, the on-time events of fluorescence intermittency for QDs on TiO_2 are more significantly suppressed than those on glass. The shortened on events are expected to be caused by the ET from QDs to the TiO_2 film. The analogous phenomena have been reported elsewhere (Hamada et al., 2010; Jin & Lian, 2009). The more rapid the ET is, the shorter the on-state lifetime becomes. The fluorescence lifetime may be estimated by (Jin & Lian, 2009; Kamat, 2008; Robel et al., 2006)

$$\tau = \frac{1}{k_r + k_A + k_{ET}} \tag{10}$$

where k_r, k_A, and k_{ET} denote intrinsic decay rate of radiation, Auger relaxation rate, and ET rate. When QD is adsorbed on glass, the ET rate is assumed to be zero. The fluorescence fluctuation is dominated by the Auger relaxation. Thus, given the lifetime measurements on both glass and TiO_2 and assumption of the same Auger relaxation rate, the ET rate constant from QDs to TiO_2 can be estimated by the reciprocal of the lifetime difference. The resulting ET rate constants are $(1.5\pm1.4)\times10^7$ and $(6.8\pm8.1)\times10^6$ s^{-1} for the QDs A and B, respectively. A large uncertainty is caused by a wide lifetime distribution. The ET rates depend on the QDs size. The smaller QDs have a twice larger rate constant. However, the ET rate constant for

the largest size cannot be determined precisely, due to a slight lifetime difference but with large uncertainty. The ET quantum yield Φ may then be estimated as 22.6 and 13.3% for the A and B sizes, respectively, according to the following equation,

$$\Phi = \frac{k_{ET}}{k_r + k_A + k_{ET}} = k_{ET}\tau \tag{11}$$

The larger QDs result in a smaller quantum yield.

In an analogous experiment, Jin and Lian obtained an average ET rate of 3.2×10^7 s^{-1} from CdSe/ZnS core/shell QDs with capped carboxylic acid functional groups (Jin & Lian, 2009). Their size was estimated to have core diameter of 4.0 nm based on the first exciton peak at 585 nm. While considering the size dependence, our result is about ten times smaller. It might be caused by the additional carboxylic acid functional groups which can speed up the ET rates.

Different from the method of lifetime measurement, autocorrelation of fluorescence intensities can be alternatively used to quantify the kinetic rate constants in on-off transition, as described in Section III.C (Chen et al., 2010). By analyzing exponential autocorrelation of fluorescence trajectory under a three-level energy system, the forward and back ET rate constants of single oxazine 1 dye/TiO_2 film were reported above (Chen et al., 2010). As the uncertainty was considered, there was no statistical difference of the lifetime measurements for the single dye adsorption between glass and TiO_2. Such a small ET activity can be indeed quantified by analyzing the autocorrelation function. Unfortunately, this method cannot be applied effectively to the QDs case, because the kinetic system involves multiple manifolds that make analysis more complicated.

The non-exponential fluorescence fluctuation was reported in single semiconductor QDs early in 1996 (Nirmal et al., 1996). To explain such fluorescence intermittency, Efros *et al.* (Efros & Rosen, 1997) proposed an Auger ionization model, in which an electron (hole) ejection outside the core QDs is caused by nonradiative relaxation of a bi-exciton. However, Auger ionization process would lead to a single exponential probability distribution of 'on' events, which is against the power-law distributions and the large dynamic range of time scale observed experimentally (Kuno et al., 2000, 2001). Nesbitt and coworkers later investigated the detailed kinetics of fluorescence intermittency in colloidal CdSe QDs and evaluated several related models at the single molecule level. They concluded that the kinetics of electron or hole tunneling to trap sites with environmental fluctuation should be more appropriate to account for the blinking phenomena (Kuno et al., 2001). Frantsuzov and Marcus (Frantsuzov & Marcus, 2005) further suggested a model regarding fluctuation of nonradiative recombination rate to account for the unanswered problem for a continuous distribution of relaxation times.

To compare the blinking activity for a single QD, probability density P(t) is defined to indicate the blinking frequency between the on and off states. The probability density P(t) of a QD at on or off states for duration time t may be calculated by(Kuno et al., 2001; Cui et al., 2008; Jin & Lian, 2009; Jin et al., 2010a)

$$P_i(t) = \frac{N_i(t)}{N_{i,tot}\Delta t_{av}} \tag{12}$$

where i denotes on or off states, N(t) the number of on or off events of duration time t, N_{tot} the total number of on or off events, and Δt_{av} the average time between the nearest neighbor events. The threshold fluorescence intensity to separate the on and off states is set at 3σ. σ is

the standard deviation of the background fluorescence intensity which can be fitted with a Gaussian function.

Fig.15 shows a fluorescence trajectory with a threshold intensity and its corresponding blinking frequency for a single QD (3.6 nm) on glass and TiO_2. The subsequent on-state and off-state probability densities accumulated over 10 single QDs for each species are displayed in Fig.16 and Fig.17, which show similar behavior as a single QD but with more data points to reduce uncertainty. The P(t) distribution at the on state for each size under either surface condition essentially follows power law statistics at the short time but deviates downward at the long time tails. The bending tail phenomena are similar to those reported (Tang & Marcus, 2005a, b; Cui et al., 2008; Peterson & Nesbitt, 2009; Jin et al., 2010a). These on-state distributions can be fitted by a truncated power law, as expressed by (Tang & Marcus, 2005a, b; Cui et al., 2008; Peterson & Nesbitt, 2009; Jin et al., 2010a)

$$P_i(t) = Dt^{-m_i} \exp(-\Gamma_i t) \tag{13}$$

where D is the amplitude associated with electronic coupling and other factors, m_i the power law exponent for the on state, and Γ the saturation rate. The truncated power law was developed by Marcus and coworkers for interpreting the blinking behavior of QD which was attributed to the ET process between a QD and its localized surface states (Tang & Marcus, 2005a, b). According to eq.13, the fitting parameters of m_{on} and Γ_{on} are listed in Table 3. The QDs on TiO_2 apparently result in larger Γ values than those on glass. In addition, the trend is found that a smaller QD may have a larger Γ. As for m_{on}, the obtained range is from 0.70 to 0.93, smaller than 1.5 as expected by Marcus model (Tang & Marcus, 2005a, b; Cui et al., 2008). Such deviation for m_{on} was also found by the Lian group in a similar experiment (Jin et al., 2010a; Jin et al., 2010b). Note that the power law distribution with a bending tail in the long time region is solely found at the on states. In contrast, the off-state probability density may be fit to a simple power law statistics expressed by,

$$P_i(t) = Et^{-m_i} \tag{14}$$

where E is a scaling coefficient and m_i is the power law exponent for the off state. A similar trend for both on- and off-state distributions was analogously found elsewhere (Cui et al., 2008; Peterson & Nesbitt, 2009). As listed in Table 3, the obtained m_{off} yields a smaller value when QDs are adsorbed on TiO_2. They lie in the range of 1.6-2.1, which are consistent with those reported (Kuno et al., 2001; Cui et al., 2008; Peterson & Nesbitt, 2009).

The on-time saturation rate should be associated with the ET rate. According to Marcus model (Tang & Marcus, 2005a, b), the free energy curves of light emitting state and dark state can be represented by an individual parabola along a reaction coordinate, which is assumed to have the same curvature. Then, Γ_{on} can be related to the free energy change ΔG_{ET} based on the ET process. That is (Tang & Marcus, 2005a, b; Cui et al., 2008),

$$\Gamma_{on} = \frac{(\lambda + \Delta G_{ET})^2}{8 t_{diff} \lambda k_B T} \tag{15}$$

where λ is the system reorganization energy, t_{diff} the diffusion correlation time constant for motion on a parabolic energy surface, k_B the Boltzmann constant, and T the absolute temperature. Given the conduction band of -4.41 eV for TiO_2 NPs and the LUMO potentials of QDs, -3.67 and -3.86 eV for the A and B sizes, respectively, the corresponding $-\Delta G_{ET}$ may

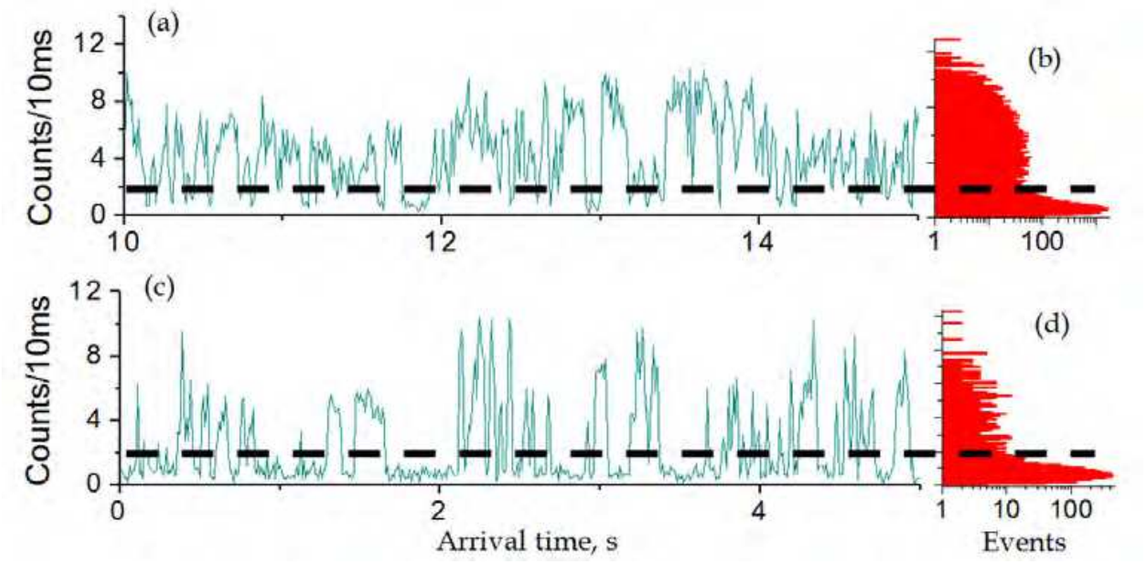

Fig. 15. The fluorescence trajectory and corresponding on/off blinking frequency distribution of single QD A on (a,b) glass and (c,d) TiO_2 film. The black lines denote the intensity thresholds to separate the on and off state which are set at a level 3σ above the background noise. σ is the standard deviation of background noise.

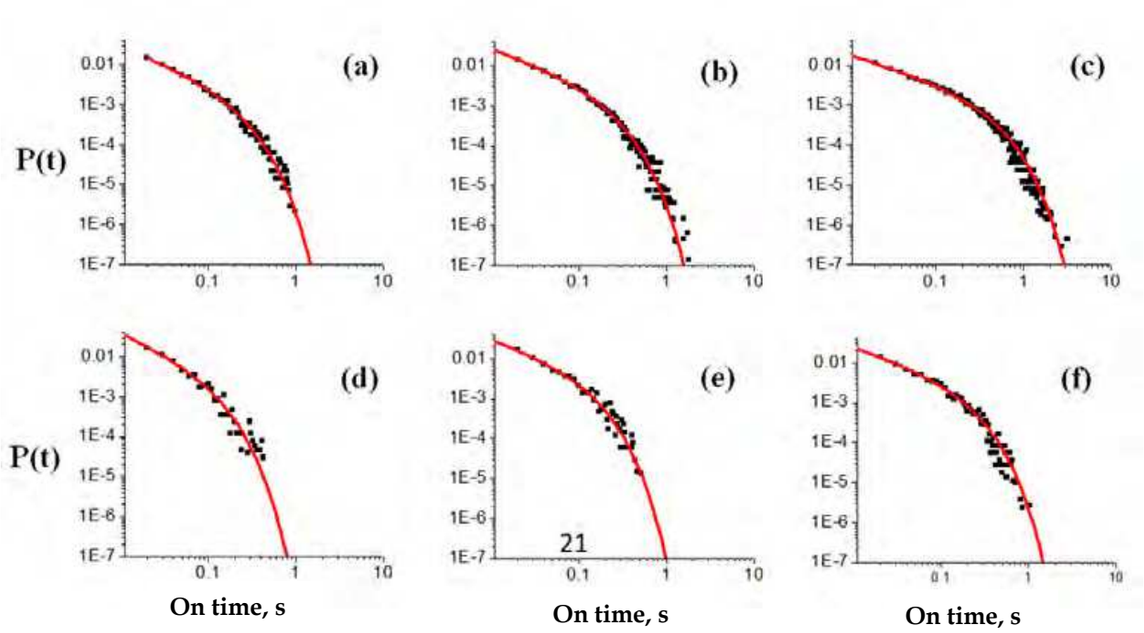

Fig. 16. The on-state probability density of 10 single QDs with A, B, and C size on (a,b,c) glass and (d,e,f) TiO_2 film. The order of increased size is followed from a to c and from d to f. The spots denote experimental data and lines denote simulation by truncated power law distribution.

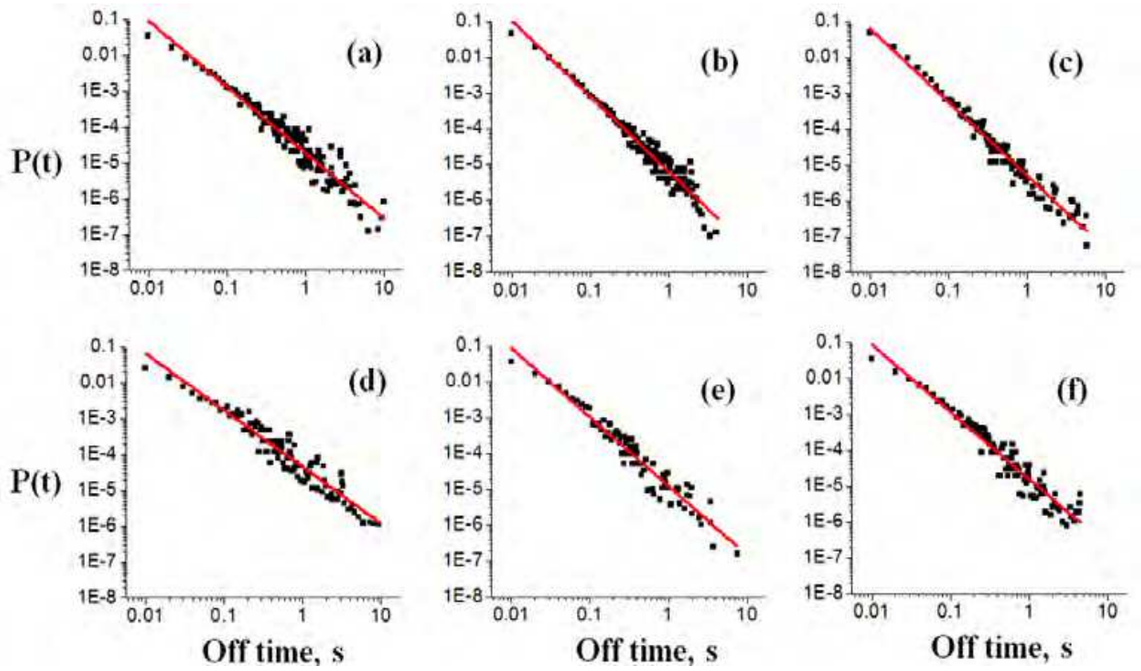

Fig. 17. The off-state probability density of 10 single QDs with A, B, and C size on (a,b,c) glass and (d,e,f) TiO_2 film. The order of increased size is followed from a to c and from d to f. The spots denote experimental data and lines denote simulation by power law distribution.

Quantum dots	Substrate	m_{on}	m_{off}	$1/\Gamma_{on}$,ms
A	Glass	0.910 ± 0.005	1.85 ± 0.04	181.9 ± 3.1
	TiO_2 film	0.925 ± 0.006	1.58 ± 0.05	75.7 ± 1.3
B	Glass	0.803 ± 0.002	2.07 ± 0.05	188.6 ± 1.9
	TiO_2 film	0.785 ± 0.005	1.91 ± 0.06	108.4 ± 2.1
C	Glass	0.699 ± 0.002	2.04 ± 0.04	355.4 ± 4.3
	TiO_2 film	0.760 ± 0.004	1.87 ± 0.05	172.0 ± 3.1

Table 3. The fitting parameters of 10 single quantum dots at the on state in terms of truncated power law distribution and off state in terms of power law distribution.

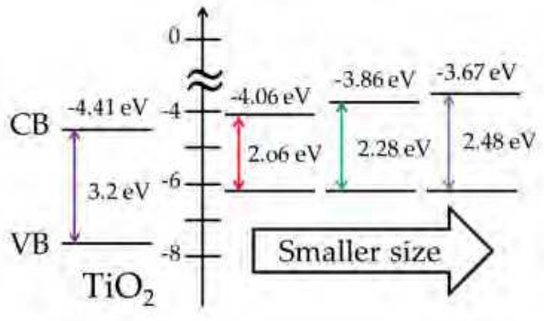

Fig. 18. The energy diagram of TiO_2 and QDs with A, B, and C size.

be estimated to be 0.74 and 0.55 eV. The related energy diagram is displayed in Fig.18. For a smaller QD, the larger conduction band gap between QD and TiO_2 can induce a larger driving force to facilitate the ET process (Tvrdy et al., 2011). If λ and t_{diff} remain constant, substituting ΔG_{ET} and Γ_{on} into eq.15 for different size of QDs yields λ to be 636 and -416 meV, of which only the positive value is meaningful.

4.3 Model prediction of electron transfer

In the following is the Marcus model which has been successfully used to describe the ET kinetics for the systems of organic dyes coupled to various metal oxides (She et al., 2005; Tvrdy et al., 2011),

$$k_{ET} = \frac{4\pi^2}{h}\int_{-\infty}^{\infty}\rho(E)\left|H(E)\right|^2\frac{1}{\sqrt{4\pi\lambda k_B T}}\exp(\frac{(1+\Delta G+E)^2}{4\lambda k_B T})dE \tag{16}$$

where H(E) is the overlap matrix element, ρ(E) the density of electron accepting states, h the Planck's constant, and ΔG the free energy change of the system, which is composed of three factors. They are (1) the energy change between initial and final electronic states, equivalent to ΔG_{ET} mentioned in eq.15, (2) the free energy difference between nonneutral donating and accepting species in the ET process, and (3) the free energy of coulombic interaction for electron and hole separation (Tvrdy et al., 2011). Among them, only ΔG_{ET} can be measured experimentally. Because of similarity as the work by the Kamat group (Tvrdy et al., 2011), the contributions of the second and third factors are referred to their work. That is,

$$\Delta G = \Delta G_{ET} + \frac{e^2}{2R_{QD}} + 2.2\frac{e^2}{\varepsilon_{QD}R_{QD}} - \frac{e^2}{4(R_{QD}+s)}\frac{\varepsilon_{TiO_2}-1}{\varepsilon_{TiO_2}+1} \tag{17}$$

where e is the elementary charge, R_{QD} and ε_{QD} are the radius and dielectric permittivity of the QD, ε_{TiO2} is the dielectric permittivity of TiO_2, and s is the separation distance between QD and TiO_2. Given s, assumed to be the same as reported (Tvrdy et al., 2011), and the data of ΔG_{ET}, R_{QD}, ε_{QD} and ε_{TiO2}, ΔG is estimated to be -0.22, -0.143, and -0.054 eV for the A, B, and C sizes of QDs, respectively. As compared to ΔG_{ET}, the driving force for moving electron from QD to TiO_2 is suppressed after taking into account the additional contributions in eq.17.

In a perfect semiconductor crystal, the density of unoccupied states ρ(E) is given as (She et al., 2005; Tvrdy et al., 2011)

$$\rho(E) = V_o\ \frac{(2m_e^*)^{3/2}}{2\pi\hbar^3}\sqrt{E} \tag{18}$$

where V_o is the effective volume, known to be 34.9 Å^3 for TiO_2 crystal, m_e^* the electron effective mass, equivalent to 10 m_0 (m_0 is the mass of free electron) (She et al., 2005), and ħ is $h/2\pi$. For a TiO_2 nanoparticle with high surface to volume ratio, the density of states in eq.18 requires modification by considering the defect states which are treated as a Gaussian distribution of width Δ. (She et al., 2005; Tvrdy et al., 2011) The modified density of states $\rho_D(E)$ is then expressed as

$$\rho_D(E) = \int_0^{\infty}\rho(E')\frac{1}{\Delta\sqrt{2\pi}}\exp(\frac{(E-E')^2}{2\Delta^2})dE' \tag{19}$$

Given a constant H(E), substituting eqs.18 and 19 into eq.16 yields an explicit relation between k_{ET} and ΔG.

As reported (She et al., 2005), when the dye/metal oxide system was surrounded by a buffer layer, the reorganization energy λ increases to 100-500 meV, because additional energy is required for system rearrangement. In this work, CdSe/ZnS QDs are spin-coated on the TiO_2 NPs film which is exposed to the air. The requirement of reorganization energy should be small. Therefore, the λ value of 636 meV in the estimate (eq.15) seems to be unreasonable. When ΔG_{ET} is replaced by ΔG, λ is obtained to be 178 and -248 meV based on eq.15. The selected λ of 178 meV is more acceptable than the one obtained with ΔG_{ET} substituted. The width Δ of defect states for the TiO_2 NPs is insensitive in the k_{ET} calculation by eq.16. We adopt the same Δ of 50 meV as reported (Tvrdy et al., 2011). Given H(E) assumed to have 0.83 cm^{-1} and the data of ΔG, λ, and Δ, k_{ET} is optimized to be 1.42×10^7, 6.80×10^6, and 1.86×10^6 s^{-1} for three increased sizes of QDs. The first two results agree very well with the experimental findings. The ET rate constant for the C type of QDs cannot be precisely determined experimentally, but may be estimated with the aid of model prediction.

For our system, CdSe/ZnS core/shell QDs are spin-coated on the TiO_2 thin film. Unlike this preparation procedure, Kamat and coworkers immersed TiO_2 film in the colloidal CdSe QDs solution to make a tight contact between donor and acceptor and then measured the electron transfer rates under a vacuum condition (Tvrdy et al., 2011). Therefore, the overlap matrix elements, H(E), which is associated with the coupling between electron donating and accepting states, must make difference. In our work, the core CdSe QD and TiO_2 have a loose contact and thus a smaller H(E) of 0.83 cm^{-1} is obtained. In contrast, a much larger value of 57 cm^{-1} was adopted by the Kamat group (Tvrdy et al., 2011). That is why the ET rates obtained herein are relatively slower by a factor of 10^4.

5. Concluding remarks

This chapter describes IFET induced by a single dye molecule or a single QD which is individually adsorbed on the TiO_2 NPs film. The fluorescence lifetimes determined among different single oxazine 1 dye molecules are widely spread, because of micro-environmental influence. These lifetimes are in proximity to those measured on the bare coverslip, indicative of the IFET inefficiency for those dye molecules sampled in this work. However, some molecules may proceed via very efficient IFET process, but fail to be detected. Due to a shorter triplet excursion, oxazine 1-TiO_2 NPs system is treated effectively as a three-level system upon irradiation. The exponential autocorrelation function may thus be analyzed to quantify the related kinetic rate constants in an on-off transition. The IFET processes are found to be inhomogeneous, with a rate constant varying from molecule to molecule. The reactivity and rate of ET fluctuation of the same single molecule are the main source to result in fluorescence intensity fluctuation. These phenomena, which are obscured in the ensemble-averaged system, are attributed to micro-environment variation for each single molecule. The oxazine 1 dye is apparently unsuitable for application to the DSSC design, because of its lower ET rates. Nevertheless, the single molecule spectroscopy provides a potential tool looking into the microscopic ET behaviors for different dye molecules to facilitate the working efficiency for the cell design. In addition, it is capable of detecting a low ET quantum yield, which is difficult to measure with conventional ensemble-averaged methods.

The second part of this chapter describes the ET from QDs to TiO_2 NPs film. The ET kinetics depends on the size of CdSe/ZnS QDs. The trajectories of fluorescence intermittency of three different sizes of QDs on glass and TiO_2 are acquired and the subsequent fluorescence lifetimes are determined. While assuming the lack of electron transfer for the QD on glass, the ET rates from QD to TiO_2 may be inferred in terms of reciprocal of the lifetime difference. The following trend is found: the smaller the size of QDs, the larger the ET rate constants. The distribution of off-time probability density versus the arrival time is fit to a simple power law statistics. However, the plot of on-time probability density can be characterized by a truncated power law distribution. Marcus's electron transfer model is employed to fit the bending tail behavior and to further calculate the ET rate constants, which show consistency with our experimental findings.

6. Acknowledgments

This work is supported by National Science Council, Taiwan, Republic of China under contract no. NSC 99-2113-M-001-025-MY3 and National Taiwan University, Ministry of Education.

7. References

Ambrose, W. P., P. M. Goodwin, J. C. Martin & R. A. Keller (1994) Single-molecule Detection and Photochemistry on a Surface Using Near-field Optical excitation. *Physical Review Letters,* 72, 1, (Jan 1994), 160-163, 0031-9007

Arden, W. & P. Fromherz (1980) Photosensitization of Semiconductor Electrode by Cyanine Dye in Lipid Bilayer. *Journal of the Electrochemical Society,* 127, 2, 1980), 370-378, 0013-4651

Baker, D. R. & P. V. Kamat (2009) Photosensitization of TiO2 Nanostructures with CdS Quantum Dots: Particulate versus Tubular Support Architectures. *Advanced Functional Materials,* 19, 5, (Mar 2009), 805-811, 1616-301X

Bell, T. D. M., C. Pagba, M. Myahkostupov, J. Hofkens & P. Piotrowiak (2006) Inhomogeneity of electron injection rates in dye-sensitized TiO2: Comparison of the mesoporous film and single nanoparticle Behavior. *Journal of Physical Chemistry B,* 110, 50, (Dec 2006), 25314-25321, 1520-6106

Biesmans, G., M. Vanderauweraer, C. Cathry & F. C. Deschryver (1992) On the Photosensitized Injection of Electrons into SNO_2 from Cyanine Dyes Incorporated in Langmuir-Blodgett-Films. *Chemical Physics,* 160, 1, (Feb 1992), 97-121, 0301-0104

Biesmans, G., M. Vanderauweraer, C. Cathry, D. Meerschaut, F. C. Deschryver, W. Storck & F. Willig (1991) Photosensitized Electron Injection from Xanthene Dyes Incorporated in Langmuir-Blodgett-Films into SNO_2 Electrodes. *Journal of Physical Chemistry,* 95, 9, (May 1991), 3771-3779, 0022-3654

Bisquert, J., A. Zaban & P. Salvador (2002) Analysis of the mechanisms of electron recombination in nanoporous TiO2 dye-sensitized solar cells. Nonequilibrium steady-state statistics and interfacial electron transfer via surface states. *Journal of Physical Chemistry B,* 106, 34, (Aug 2002), 8774-8782, 1520-6106

Cahen, D., G. Hodes, M. Gratzel, J. F. Guillemoles & I. Riess (2000) Nature of photovoltaic action in dye-sensitized solar cells. *Journal of Physical Chemistry B,* 104, 9, (Mar 2000), 2053-2059, 1089-5647

Chen, Y. J., H. Y. Tzeng, H. F. Fan, M. S. Chen, J. S. Huang & K. C. Lin (2010) Photoinduced Electron Transfer of Oxazine 1/TiO2 Nanoparticles at Single Molecule Level by Using Confocal Fluorescence Microscopy. *Langmuir,* 26, 11, (Jun 2010), 9050-9060, 0743-7463

Choi, J. J., Y. F. Lim, M. B. Santiago-Berrios, M. Oh, B. R. Hyun, L. F. Sung, A. C. Bartnik, A. Goedhart, G. G. Malliaras, H. D. Abruna, F. W. Wise & T. Hanrath (2009) PbSe Nanocrystal Excitonic Solar Cells. *Nano Letters,* 9, 11, (Nov 2009), 3749-3755, 1530-6984

Cotlet, M., S. Masuo, G. B. Luo, J. Hofkens, M. Van der Auweraer, J. Verhoeven, K. Mullen, X. L. S. Xie & F. De Schryver (2004) Probing conformational dynamics in single donor-acceptor synthetic molecules by means of photoinduced reversible electron transfer. *Proceedings of the National Academy of Sciences of the United States of America,* 101, 40, (Oct 2004), 14343-14348, 0027-8424

Cotlet, M., T. Vosch, S. Habuchi, T. Weil, K. Mullen, J. Hofkens & F. De Schryver (2005) Probing intramolecular Forster resonance energy transfer in a naphthaleneimide-peryleneimide-terrylenediimide-based dendrimer by ensemble and single-molecule fluorescence spectroscopy. *Journal of the American Chemical Society,* 127, 27, (Jul 2005), 9760-9768, 0002-7863

Cui, S. C., T. Tachikawa, M. Fujitsuka & T. Majima (2008) Interfacial Electron Transfer Dynamics in a Single CdTe Quantum Dot-Pyromellitimide Conjugate. *Journal of Physical Chemistry C,* 112, 49, (Dec 2008), 19625-19634, 1932-7447

Efros, A. L. & M. Rosen (1997) Random telegraph signal in the photoluminescence intensity of a single quantum dot. *Physical Review Letters,* 78, 6, (Feb 1997), 1110-1113, 0031-9007

Fan, S. Q., B. Fang, J. H. Kim, J. J. Kim, J. S. Yu & J. Ko (2010) Hierarchical nanostructured spherical carbon with hollow core/mesoporous shell as a highly efficient counter electrode in CdSe quantum-dot-sensitized solar cells. *Applied Physics Letters,* 96, 6, (Feb 2010), 0003-6951

Ferrere, S. & B. A. Gregg (2001) Large increases in photocurrents and solar conversion efficiencies by UV illumination of dye sensitized solar cells. *Journal of Physical Chemistry B,* 105, 32, (Aug 2001), 7602-7605, 1089-5647

Flors, C., I. Oesterling, T. Schnitzler, E. Fron, G. Schweitzer, M. Sliwa, A. Herrmann, M. van der Auweraer, F. C. de Schryver, K. Mullen & J. Hofkens (2007) Energy and electron transfer in ethynylene bridged perylene diimide multichromophores. *Journal of Physical Chemistry C,* 111, 12, (Mar 2007), 4861-4870, 1932-7447

Frantsuzov, P. A. & R. A. Marcus (2005) Explanation of quantum dot blinking without the long-lived trap hypothesis. *Physical Review B,* 72, 15, (Oct 2005), 1098-0121

Gaiduk, A., R. Kuhnemuth, S. Felekyan, M. Antonik, W. Becker, V. Kudryavtsev, C. Sandhagen & C. A. M. Seidel (2007) Fluorescence detection with high time resolution: From optical microscopy to simultaneous force and fluorescence

spectroscopy. *Microscopy Research and Technique,* 70, 5, (May 2007), 433-441, 1059-910X

Garcia-Parajo, M. F., G. M. J. Segers-Nolten, J. A. Veerman, J. Greve & N. F. van Hulst (2000) Real-time light-driven dynamics of the fluorescence emission in single green fluorescent protein molecules. *Proceedings of the National Academy of Sciences of the United States of America,* 97, 13, (Jun 2000), 7237-7242, 0027-8424

Gratzel, M. (2001) Photoelectrochemical cells. *Nature,* 414, 6861, (Nov 2001), 338-344, 0028-0836

Gratzel, M. (2003) Dye-sensitized solar cells. *Journal of Photochemistry and Photobiology C-Photochemistry Reviews,* 4, 2, (Oct 2003), 145-153, 1389-5567

Gratzel, M. (2005) Mesoscopic solar cells for electricity and hydrogen production from sunlight. *Chemistry Letters,* 34, 1, (Jan 2005), 8-13, 0366-7022

Haase, M., C. G. Hubner, E. Reuther, A. Herrmann, K. Mullen & T. Basche (2004) Exponential and power-law kinetics in single-molecule fluorescence intermittency. *Journal of Physical Chemistry B,* 108, 29, (Jul 2004), 10445-10450, 1520-6106

Hagfeldt, A. & M. Gratzel (2000) Molecular photovoltaics. *Accounts of Chemical Research,* 33, 5, (May 2000), 269-277, 0001-4842

Hamada, M., S. Nakanishi, T. Itoh, M. Ishikawa & V. Biju (2010) Blinking Suppression in CdSe/ZnS Single Quantum Dots by TiO2 Nanoparticles. *Acs Nano,* 4, 8, (Aug 2010), 4445-4454, 1936-0851

Hara, K., H. Horiuchi, R. Katoh, L. P. Singh, H. Sugihara, K. Sayama, S. Murata, M. Tachiya & H. Arakawa (2002) Effect of the ligand structure on the efficiency of electron injection from excited Ru-phenanthroline complexes to nanocrystalline TiO2 films. *Journal of Physical Chemistry B,* 106, 2, (Jan 2002), 374-379, 1520-6106

Hartmann, T., V. I. Yudson & P. Reineker (2011) Model for the off-time distribution in blinking quantum dots. *Journal of Luminescence,* 131, 3, 2011), 379-381, 0022-2313

Holman, M. W. & D. M. Adams (2004) Using single-molecule fluorescence spectroscopy to study electron transfer. *ChemPhysChem,* 5, 12, (Dec 2004), 1831-1836, 1439-4235

Jin, S. Y., J. C. Hsiang, H. M. Zhu, N. H. Song, R. M. Dickson & T. Q. Lian (2010a) Correlated single quantum dot blinking and interfacial electron transfer dynamics. *Chemical Science,* 1, 4, (Oct 2010a), 519-526, 2041-6520

Jin, S. Y. & T. Q. Lian (2009) Electron Transfer Dynamics from Single CdSe/ZnS Quantum Dots to TiO2 Nanoparticles. *Nano Letters,* 9, 6, (Jun 2009), 2448-2454, 1530-6984

Jin, S. Y., N. H. Song & T. Q. Lian (2010b) Suppressed Blinking Dynamics of Single QDs on ITO. *Acs Nano,* 4, 3, (Mar 2010b), 1545-1552, 1936-0851

Ju, T., R. L. Graham, G. M. Zhai, Y. W. Rodriguez, A. J. Breeze, L. L. Yang, G. B. Alers & S. A. Carter (2010) High efficiency mesoporous titanium oxide PbS quantum dot solar cells at low temperature. *Applied Physics Letters,* 97, 4, (Jul 2010), 0003-6951

Kamat, P. V. (2008) Quantum Dot Solar Cells. Semiconductor Nanocrystals as Light Harvesters. *Journal of Physical Chemistry C,* 112, 48, (Dec 2008), 18737-18753, 1932-7447

Kim, S. J., W. J. Kim, Y. Sahoo, A. N. Cartwright & P. N. Prasad (2008) Multiple exciton generation and electrical extraction from a PbSe quantum dot photoconductor. *Applied Physics Letters,* 92, 3, (Jan 2008), 0003-6951

Kohn, F., J. Hofkens, R. Gronheid, M. Van der Auweraer & F. C. De Schryver (2002) Parameters influencing the on- and off-times in the fluorescence intensity traces of single cyanine dye molecules. *Journal of Physical Chemistry A,* 106, 19, (May 2002), 4808-4814, 1089-5639

Krauss, T. D. & J. J. Peterson (2010) Bright Future for Fluorescence Blinking in Semiconductor Nanocrystals. *Journal of Physical Chemistry Letters,* 1, 9, (May 2010), 1377-1382, 1948-7185

Kulzer, F., S. Kummer, R. Matzke, C. Brauchle & T. Basche (1997) Single-molecule optical switching of terrylene in p-terphenyl. *Nature,* 387, 6634, (Jun 1997), 688-691, 0028-0836

Kuno, M., D. P. Fromm, H. F. Hamann, A. Gallagher & D. J. Nesbitt (2000) Nonexponential "blinking" kinetics of single CdSe quantum dots: A universal power law behavior. *Journal of Chemical Physics,* 112, 7, (Feb 2000), 3117-3120, 0021-9606

Kuno, M., D. P. Fromm, H. F. Hamann, A. Gallagher & D. J. Nesbitt (2001) "On"/"off" fluorescence intermittency of single semiconductor quantum dots. *Journal of Chemical Physics,* 115, 2, (Jul 2001), 1028-1040, 0021-9606

Lee, Y. L. & Y. S. Lo (2009) Highly Efficient Quantum-Dot-Sensitized Solar Cell Based on Co-Sensitization of CdS/CdSe. *Advanced Functional Materials,* 19, 4, (Feb 2009), 604-609, 1616-301X

Luther, J. M., M. C. Beard, Q. Song, M. Law, R. J. Ellingson & A. J. Nozik (2007) Multiple exciton generation in films of electronically coupled PbSe quantum dots. *Nano Letters,* 7, 6, (Jun 2007), 1779-1784, 1530-6984

Luther, J. M., M. Law, M. C. Beard, Q. Song, M. O. Reese, R. J. Ellingson & A. J. Nozik (2008) Schottky Solar Cells Based on Colloidal Nanocrystal Films. *Nano Letters,* 8, 10, (Oct 2008), 3488-3492, 1530-6984

Michalet, X., S. Weiss & M. Jager (2006) Single-molecule fluorescence studies of protein folding and conformational dynamics. *Chemical Reviews,* 106, 5, (May 2006), 1785-1813, 0009-2665

Moerner, W. E. & D. P. Fromm (2003) Methods of single-molecule fluorescence spectroscopy and microscopy. *Review of Scientific Instruments,* 74, 8, (Aug 2003), 3597-3619, 0034-6748

Nirmal, M., B. O. Dabbousi, M. G. Bawendi, J. J. Macklin, J. K. Trautman, T. D. Harris & L. E. Brus (1996) Fluorescence intermittency in single cadmium selenide nanocrystals. *Nature,* 383, 6603, (Oct 1996), 802-804, 0028-0836

Oregan, B. & M. Gratzel (1991) A Low-cost, High-efficiency Solar-cell Based on Dye-sensitized Colloidal TiO_2 Films. *Nature,* 353, 6346, (Oct 1991), 737-740, 0028-0836

Peterson, J. J. & D. J. Nesbitt (2009) Modified Power Law Behavior in Quantum Dot Blinking: A Novel Role for Biexcitons and Auger Ionization. *Nano Letters,* 9, 1, (Jan 2009), 338-345, 1530-6984

Plass, R., S. Pelet, J. Krueger, M. Gratzel & U. Bach (2002) Quantum dot sensitization of organic-inorganic hybrid solar cells. *Journal of Physical Chemistry B,* 106, 31, (Aug 2002), 7578-7580, 1520-6106

Ramakrishna, G., D. A. Jose, D. K. Kumar, A. Das, D. K. Palit & H. N. Ghosh (2005) Strongly coupled ruthenium-polypyridyl complexes for efficient electron injection in dye-

sensitized semiconductor nanoparticles. *Journal of Physical Chemistry B,* 109, 32, (Aug 2005), 15445-15453, 1520-6106

Robel, I., V. Subramanian, M. Kuno & P. V. Kamat (2006) Quantum dot solar cells. Harvesting light energy with CdSe nanocrystals molecularly linked to mesoscopic TiO2 films. *Journal of the American Chemical Society,* 128, 7, (Feb 2006), 2385-2393, 0002-7863

Sambur, J. B., T. Novet & B. A. Parkinson (2010) Multiple Exciton Collection in a Sensitized Photovoltaic System. *Science,* 330, 6000, (Oct 2010), 63-66, 0036-8075

Sens, R. & K. H. Drexhage (1981) Fluorescence Quantum Yield of Oxazine and Carbazine Laser-dyes. *Journal of Luminescence,* 24-5, NOV, 1981), 709-712, 0022-2313

She, C. X., N. A. Anderson, J. C. Guo, F. Liu, W. H. Goh, D. T. Chen, D. L. Mohler, Z. Q. Tian, J. T. Hupp & T. Q. Lian (2005) pH-dependent electron transfer from re-bipyridyl complexes to metal oxide nanocrystalline thin films. *Journal of Physical Chemistry B,* 109, 41, (Oct 2005), 19345-19355, 1520-6106

Tang, J. & R. A. Marcus (2005a) Diffusion-controlled electron transfer processes and power-law statistics of fluorescence intermittency of nanoparticles. *Physical Review Letters,* 95, 10, (Sep 2005a), 0031-9007

Tang, J. & R. A. Marcus (2005b) Mechanisms of fluorescence blinking in semiconductor nanocrystal quantum dots. *Journal of Chemical Physics,* 123, 5, (Aug 2005b), 0021-9606

Tvrdy, K., P. A. Frantsuzov & P. V. Kamat (2011) Photoinduced electron transfer from semiconductor quantum dots to metal oxide nanoparticles. *Proceedings of the National Academy of Sciences of the United States of America,* 108, 1, (Jan 2011), 29-34, 0027-8424

VandenBout, D. A., W. T. Yip, D. H. Hu, D. K. Fu, T. M. Swager & P. F. Barbara (1997) Discrete intensity jumps and intramolecular electronic energy transfer in the spectroscopy of single conjugated polymer molecules. *Science,* 277, 5329, (Aug 1997), 1074-1077, 0036-8075

Veerman, J. A., M. F. Garcia-Parajo, L. Kuipers & N. F. van Hulst (1999) Time-varying triplet state lifetimes of single molecules. *Physical Review Letters,* 83, 11, (Sep 1999), 2155-2158, 0031-9007

Wang, Y. M., X. F. Wang, S. K. Ghosh & H. P. Lu (2009) Probing Single-Molecule Interfacial Electron Transfer Dynamics of Porphyrin on TiO2 Nanoparticles. *Journal of the American Chemical Society,* 131, 4, (Feb 2009), 1479-1487, 0002-7863

Wilkinson, F., G. P. Kelly, L. F. V. Ferreira, V. Freire & M. I. Ferreira (1991) Benzophenone Sensitization of Triplet Oxazine and of Delayed Fluorescence by Oxazine in Acetonitrile Solution. *Journal of the Chemical Society-Faraday Transactions,* 87, 4, (Feb 1991), 547-552, 0956-5000

Xie, X. S. & R. C. Dunn (1994) Probing Single-molecule Dynamics. *Science,* 265, 5170, (Jul 1994), 361-364, 0036-8075

Yip, W. T., D. H. Hu, J. Yu, D. A. Vanden Bout & P. F. Barbara (1998) Classifying the photophysical dynamics of single- and multiple-chromophoric molecules by single molecule spectroscopy. *Journal of Physical Chemistry A,* 102, 39, (Sep 1998), 7564-7575, 1089-5639

Yu, P. R., K. Zhu, A. G. Norman, S. Ferrere, A. J. Frank & A. J. Nozik (2006) Nanocrystalline TiO2 solar cells sensitized with InAs quantum dots. *Journal of Physical Chemistry B,* 110, 50, (Dec 2006), 25451-25454, 1520-6106

Yu, W. W., L. H. Qu, W. Z. Guo & X. G. Peng (2003) Experimental determination of the extinction coefficient of CdTe, CdSe, and CdS nanocrystals. *Chemistry of Materials,* 15, 14, (Jul 2003), 2854-2860, 0897-4756

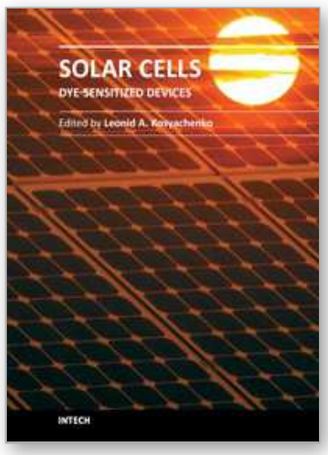

Solar Cells - Dye-Sensitized Devices
Edited by Prof. Leonid A. Kosyachenko

ISBN 978-953-307-735-2
Hard cover, 492 pages
Publisher InTech
Published online 09, November, 2011
Published in print edition November, 2011

The second book of the four-volume edition of "Solar cells" is devoted to dye-sensitized solar cells (DSSCs), which are considered to be extremely promising because they are made of low-cost materials with simple inexpensive manufacturing procedures and can be engineered into flexible sheets. DSSCs are emerged as a truly new class of energy conversion devices, which are representatives of the third generation solar technology. Mechanism of conversion of solar energy into electricity in these devices is quite peculiar. The achieved energy conversion efficiency in DSSCs is low, however, it has improved quickly in the last years. It is believed that DSSCs are still at the start of their development stage and will take a worthy place in the large-scale production for the future.

How to reference
In order to correctly reference this scholarly work, feel free to copy and paste the following:

King-Chuen Lin and Chun-Li Chang (2011). Photo-Induced Electron Transfer from Dye or Quantum Dot to TiO2 Nanoparticles at Single Molecule Level, Solar Cells - Dye-Sensitized Devices, Prof. Leonid A. Kosyachenko (Ed.), ISBN: 978-953-307-735-2, InTech, Available from: http://www.intechopen.com/books/solar-cells-dye-sensitized-devices/photo-induced-electron-transfer-from-dye-or-quantum-dot-to-tio2-nanoparticles-at-single-molecule-lev

INTECH
open science | open minds

InTech Europe
University Campus STeP Ri
Slavka Krautzeka 83/A
51000 Rijeka, Croatia
Phone: +385 (51) 770 447
Fax: +385 (51) 686 166
www.intechopen.com

InTech China
Unit 405, Office Block, Hotel Equatorial Shanghai
No.65, Yan An Road (West), Shanghai, 200040, China
中国上海市延安西路65号上海国际贵都大饭店办公楼405单元
Phone: +86-21-62489820
Fax: +86-21-62489821

IntechOpen